Dynamics of Membrane-Skeleton (Fodrin) Organization during Development of Polarity in Madin-Darby Canine Kidney Epithelial Cells

W. James Nelson and Pamela J. Veshnock

Institute for Cancer Research, Philadelphia, Pennsylvania 19111

Abstract. Madin-Darby canine kidney (MDCK) epithelial cells exhibit a polarized distribution of membrane proteins between the apical and basolateral domains of the plasma membrane. We have initiated studies to investigate whether the spectrin-based membrane skeleton plays a role in the establishment and maintenance of these membrane domains. MDCK cells express an isoform of spectrin composed of two subunits, M_r 240,000 (α-subunit) and M_r 235,000 (γ-subunit). This isoform is immunologically and structurally related to fodrin in lens and brain cells, which is a functional and structural analog of αβ-spectrin, the major component of the erythrocyte membrane skeleton. Analysis of fodrin in MDCK cells by immunoblotting, immunofluorescence, and metabolic labeling revealed significant changes in the biophysical properties, subcellular distribution, steady-state levels, and turnover of the protein during development of a continuous monolayer of cells. The changes in the cellular organization of fodrin did not appear to coincide with the distributions of microfilaments, microtubules, or intermediate filaments. These changes result in the formation of a highly insoluble, relatively dense and stable layer of fodrin which appears to be localized to the cell periphery and predominantly in the region of the basolateral plasma membrane of MDCK cells in continuous monolayers. The formation of this structure coincides temporally and spatially with extensive cell-cell contact, and with the development of the polarized distribution of the Na^+, K^+-ATPase, a marker protein of the basolateral plasma membrane.

MANY differentiated cells have a polarized organization characterized by the regionalization of proteins into discrete domains on the plasma membrane. Cells of transporting epithelia exhibit both structural and functional polarity, which is reflected in the asymmetric distribution of enzymes and transport activities between the apical and basolateral domains of the plasma membrane (17, 18, 32, 61, 83, 90). The establishment and maintenance of this polarity is critical to the function of these cells as selective permeability barriers.

Recently, there has been significant progress in dissecting the pathway(s) of protein targeting to the plasma membrane of polarized epithelial cells, which has increased our understanding of how membrane domains are established (56, 60, 75, 79; for reviews see references 81 and 86). However, little is known about the mechanism(s) involved in maintaining the asymmetric distribution of proteins upon establishment of different membrane domains. While membrane proteins are, in general, capable of lateral diffusion in the plane of the lipid bilayer (reviewed in reference 58), the extensive molecular and functional order in the plasma membrane of polarized epithelial cells indicates the presence of mechanisms to prevent proteins of different domains from mixing. Such constraints to the lateral diffusion of proteins in the membrane may be brought about passively by physical barriers such as the tight junction (zonula occludens) (25, 31, 52, 57, 72, 76, 84), which delineates the border between the apical and basolateral domains of the plasma membrane (19, 31, 32, 34, 59). Alternatively, long-range protein-protein interactions between integral membrane proteins and structural proteins in the subcortical cytoplasm may actively prevent mixing of membrane proteins through the formation of topographically fixed higher-ordered structures on the membrane.

Such higher-ordered structures have been extensively characterized in the erythrocyte (for reviews, see references 5, 15, and 20). Studies have shown that an elaborate cytoplasmic lattice of proteins (the membrane skeleton), comprised mostly of actin and spectrin (53), is attached to integral membrane proteins through specific protein interactions between spectrin-ankyrin-the anion channel protein (7-9, 89), and spectrin-band 4.1-glycophorin (1, 2). These interactions provide tensile strength to the membrane (reviewed in references 5, 15, and 20) and result in the immobilization of the integral membrane proteins in the plane of the lipid bilayer (23, 30, 85). Recently, functional and structural analogs of spectrin (termed fodrin), ankyrin, and band 4.1 have been described and characterized in a variety of nonerythroid cells (reviewed in references 5, 10, 16, 29, 30, and 68). Although

the function(s) of these analogs in nonerythroid cell organization is poorly understood, it may be significant that their distribution on the membrane of neurons (3, 21, 46, 47, 67), skeletal muscle (65), and other cells (22, 29, 51, 69, 73, 77) is nonrandom, suggesting that these proteins may play a role in establishing and maintaining membrane domains in differentiated cells (68).

We have initiated a study of the role of fodrin in cell organization using Madin-Darby Canine Kidney (MDCK)[1] cells as a model system of functionally and structurally polarized epithelial cells in culture (17, 18, 32, 61, 83, 90). Our results show that there are dramatic changes in the regulation of fodrin assembly, subcellular distribution and interaction with the membrane during the development of polarity in cultures of MDCK cells. Furthermore, these changes in the organization of the fodrin-based membrane skeleton coincide temporally and spatially with the development of the polarized distribution of the Na^+, K^+-ATPase, a marker of the basolateral domain of the plasma membrane.

Materials and Methods

Cells

MDCK cells were purchased from the American Type Culture Collection (Rockville, MD) (55). The original stock of MDCK cells (passage #53) was expanded in culture to approximately passage #58, and aliquots were frozen and stored in liquid nitrogen. One aliquot was thawed and cloned by limiting dilution in 96-well plates. Single cell clones were expanded by serial passage, and frozen and stored in liquid nitrogen (approximate passage #162). Clone 8 was used in all subsequent experiments. This clone exhibits morphological and functional polarity characteristic of these cells. (*a*) The cells exhibit morphological polarity characterized by the presence of microvilli on the apical membrane, zonula occludens at the apex of the lateral membranes, and zonula adherens and numerous desmosomes on the lateral membrane (see Fig. 1). (*b*) The cells form fluid-filled cysts in suspension culture with apical membranes on the outside (data not shown; see reference 82), and form fluid-filled cysts with the reverse polarity in a collagen matrix (data not shown); on solid or permeable substrata, the cells form discrete colonies which coalesce to form a confluent monolayer of cells in which there are no cell divisions (see Fig. 1). (*c*) The cells exhibit a functional response to hormones and compounds that elevate intracellular cAMP levels which is characterized by the formation of domes (data not shown; see reference 90). And (*d*) the cells exhibit a polarity in the distribution of membrane proteins as characterized by the asymmetric distribution of the Na^+, K^+-ATPase on the basolateral membrane (see Fig. 10).

For experimentation, cells were grown on collagen-coated 0.45-μm nitrocellulose filters (Millipore/Continental Water Systems, Bedford, MA) or collagen-coated plastic petri dishes in Dulbecco's modified Eagle's medium supplemented with 10% fetal bovine serum at 37°C in a 5% CO_2 in air, humidified atmosphere; collagen was prepared from rat tails as described previously (70). Aliquots of clone 8 were used for 4 wk and then replaced with a new replicate vial of cells from the liquid nitrogen bank. Cells were maintained at low density, subcultured by trypsinization with a solution containing 0.04% (wt/vol) trypsin and 3 mM EDTA, and plated at a density of 1×10^4–1.5×10^4 cells/cm^2 to produce a culture of single, well-spread cells after 12 h. After 72–96 h cultures of 20-cell colonies were produced, and after ~144 h a confluent monolayer of cells was formed (see Fig. 1). The culture media was changed routinely every 48 h, and 6–12 h before an experiment. The amount of DNA in the culture was determined by the method described by Labarca and Paigen (42) using a Perkin-Elmer PE-3 fluorimeter; lambda DNA was used as a standard.

1. *Abbreviations used in this paper*: DTT, dithiothreitol; MDCK, Madin-Darby canine kidney; MEM-Met, minimum essential medium without methionine and supplemented with 2.5% fetal bovine serum; PMSF, phenylmethylsulfonyl fluoride; Tris-saline, Tris-buffered saline.

Antibodies

Monospecific, polyclonal antisera have been raised in rabbits against α-fodrin, γ-fodrin, actin, vimentin, cytokeratins 8 and 18, and the α- and β-subunits of the Na^+, K^+-ATPase. α- and γ-fodrin and vimentin were isolated from calf lens membranes. Briefly, membranes were prepared by disrupting a decapsulated lens in 50 vol of a buffer containing 15 mM Tris-HCl, pH 7.5, 25 mM KCl, 2.5 mM $MgCl_2$, 0.1 mM dithiothreitol (DTT), 1 mM phenylmethylsulfonyl fluoride (PMSF) (TKM buffer) with 10 strokes in an all-glass Dounce homogenizer; all operations were performed at 4°C. Membranes were collected by centrifugation at 16,000 *g* for 10 min. The membranes were resuspended in TKM buffer, homogenized, and centrifuged as above; this procedure was repeated twice.

For the isolation of fodrin, lens membranes were solubilized by boiling in a buffer comprising 2% (wt/vol) SDS, 10 mM Tris-HCl, pH 6.8, 0.5 mM DTT, 7.5% glycerol, 2 mM EDTA (SDS sample buffer), and the proteins were separated on an SDS/5% polyacrylamide gel (43). The gel was stained briefly with Coomassie Brilliant Blue, destained, and the bands corresponding to α- and γ-fodrin, respectively, were excised from the polyacrylamide gel and equilibrated in 15 mM sodium phosphate buffer, pH 7.2, 120 mM NaCl (PBS).

Vimentin was extracted from lens membranes with a solution containing 10 mM Tris-HCl, pH 8, 1 mM EGTA, and 6 mM 2-mercaptoethanol. The extract was concentrated by $(NH_4)_2SO_4$ precipitation at 25% saturation and vimentin was purified by affinity chromatography on single-stranded DNA cellulose as described (63).

Actin was partially purified from porcine stomach smooth muscle as described (24); the final purification step was SDS PAGE as described above.

Cytokeratins were isolated from desmosomes of bovine muzzle as described (62). The cytokeratins with relative molecular masses (M_r's) of 58,000 and 52,000 were purified by SDS PAGE as described above.

The Na^+, K^+-ATPase was purified from canine kidney outer medulla as described by Jørgensen (36). The purified enzyme comprised two subunits, the catalytic α-subunit (M_r ~100,000) and a glycosylated β-subunit (M_r ~60,000). The subunits were purified by SDS PAGE (see above).

The gel slices containing each protein were homogenized in PBS, and the resulting fine gel suspension was emulsified with an equal volume of Freund's complete adjuvant. New Zealand white rabbits were injected subcutaneously with each immunogen at multiple sites along the back. Each rabbit received initially ~50–75 μg antigen, and ~35–50 μg for the booster injections using Freund's incomplete adjuvant which were given subsequently at 3-wk intervals. Blood was collected before the first injection (preimmune serum), and then 1 wk after each booster injection; bleeds after the third or fourth booster injection were used. The IgG fraction of the antisera was precipitated with $(NH_4)_2SO_4$ at 50% saturation. Antiserum raised against bovine brain tubulin was purchased from Cappel Laboratories (Cochranville, PA).

Immunoblotting

Proteins were transferred electrophoretically from SDS polyacrylamide gels to nitrocellulose filters by a modification of the method described by Towbin et al. (88). Briefly, proteins were transferred for 4 h at 0.25 A constant current in a buffer comprised of 20 mM Tris-acetate, pH 8.3, 0.1% (wt/vol) SDS, 20% (vol/vol) isopropanol. Filters were washed sequentially at room temperature in 50% (vol/vol) isopropanol (30 min); 15 mM Tris-HCl, pH 7.5, 120 mM NaCl, 5 mM NaN_3, 1 mM EDTA, 0.1% (vol/vol) Tween 20 (30 min); and 15 mM Tris-HCl, pH 7.5, 120 mM NaCl, 5 mM NaN_3, 1 mM EDTA, 0.1% (vol/vol) Tween 20, 0.1% (wt/vol) gelatin (gelatin wash buffer; overnight incubation at 30°C). Filters were incubated with a 1:1,000 dilution of the primary antiserum in gelatin wash buffer for 4 h, followed by 6–8 changes of gelatin wash buffer for ~3–4 h. Filters were then incubated with ^{125}I-protein A for 4 h. The ^{125}I-protein A was prepared as follows: 20 μg protein A (Miles Scientific Div., Naperville, IL) were incubated for 15 min at room temperature with 1 mCi ^{125}I-Na (ICN K&K Laboratories, Inc., Plainview, NY) in a vol of 100 μl containing 10 mM Tris-HCl, pH 7.5, 1 mM EDTA, 120 mM NaCl in a polypropylene tube coated with 10 μg Iodogen (Pierce Chemical Co., Rockford, IL). ^{125}I-labeled protein A was separated from free ^{125}I by gel filtration on a 5-ml column of Sephadex G-25 equilibrated in the same buffer containing, in addition, 10 mM 2-mercaptoethanol. The specific activity of the ^{125}I-protein A was ~10 μCi/μg protein A. After incubation with ^{125}I-protein A, filters were washed with 6–8 changes of gelatin wash buffer for 3–4 h, dried and exposed at −80°C to XAR-5 x-ray film preflashed to an absorbance of ~0.15 at 514 nm (45). For quantitation, the resulting autoradiograms were analyzed with a Beckman DU-7 spectrophotometer equipped with a scanning densitometer; alter-

natively, the areas of the filter corresponding to the proteins of interest were excised and the amount of ^{125}I determined directly in a γ-counter. A fivefold range of protein concentrations were analyzed with each antisera to determine that the amount of protein in each sample was within the linear range of detection by immunoblotting.

Metabolic Labeling and Immunoprecipitation

Cultures of MDCK cells were rinsed twice with minimum essential medium without methionine and supplemented with 2.5% fetal bovine serum that had been dialyzed extensively against PBS (MEM-Met). The cells were preincubated in 3 ml MEM-Met for 15 min at 37°C. The medium was discarded, and the cells were incubated at 37°C for 15 min in 500 μl MEM-Met containing 120 μCi [^{35}S]methionine (New England Nuclear, Boston, MA; ~1,200 Ci/mmol). The radioactive medium was discarded, and the cells were rinsed twice in Dulbecco's modified Eagle's medium/fetal bovine serum containing 2 mM methionine (chase medium). The cells were incubated at 37°C in 3 ml chase medium for different periods of time. At given times, the cells were placed on ice and rinsed twice with ice cold buffer containing 15 mM Tris-HCl, pH 7.5, 120 mM NaCl, 1 mM PMSF (Tris-saline). At 4°C, the cells were scraped from the petri dish in 1 ml Tris-saline using a rubber policeman, and pelleted at 12,000 *g* for 5 min. The cells were solubilized in 100 μl buffer containing 1% (wt/vol) SDS, 5 mM EDTA, 2 mM EGTA, 0.1 mM DTT, 1 mM PMSF, 10 mM Tris-HCl, pH 7.5 by boiling for 3 min. The samples were diluted 1:10 with a buffer containing 15 mM Tris-HCl, pH 7.5, 5 mM EDTA, 2 mM EGTA, 1% (vol/vol) Triton X-100, 1% (wt/vol) Na-deoxycholate, 0.1% (wt/vol) SDS, 120 mM NaCl, 25 mM KCl, 0.1 mM DTT (HS buffer), and centrifuged at 48,000 *g* for 10 min. The supernatants were transferred to clean tubes and precleared by incubation for 45 min in the presence of 10 μl preimmune serum and 50 μl of a 10% suspension of formalin-fixed protein A-bearing *Staphylococcus aureus* (Calbiochem-Behring Corp., La Jolla, CA). After centrifugation at 12,000 *g* for 5 min, the supernatants were transferred to clean tubes, and 4 μl α-fodrin or 10 μl γ-fodrin antisera was added. The samples were turned end-over-end overnight at 4°C. Immune-complexes were isolated by the addition of 20 μl of a 1:1 suspension of protein A-Sepharose 4B beads (Pharmacia Fine Chemicals, Piscataway, NJ) in HS buffer for 2 h. The beads were pelleted at 12,000 *g* for 1 min and resuspended by vortexing in 900 μl HS buffer. The suspension was underlayered with 200 μl of a solution of 1 M sucrose in HS buffer and recentrifuged as above. This procedure was repeated three times. The immunoprecipitates were removed from the beads by boiling for 3 min in 60 μl SDS sample buffer. The suspension was applied to an SDS/5% polyacrylamide gel. After electrophoresis, the gel was fixed overnight in a solution containing 50% ethanol and 10% acetic acid. The gels were soaked in dimethyl sulfoxide (two changes of 30 min each), then in a solution of 20% (wt/vol) 2,5-diphenyloxazol in dimethyl sulfoxide for 3 h, and finally washed in dH_2O for 60 min (13). The gel was dried under vacuum, and exposed at −80°C to XAR-5 x-ray film preflashed to an absorbance of ~0.15 at 514 nm (61). The resulting fluorograms are analyzed with a Beckman DU-7 spectrophotometer equipped with a scanning densitometer.

Solubility Properties of Spectrin and Vimentin from MDCK Cells and Canine Lens Plasma Membranes

Cultures of MDCK cells comprising either single cells, 20-cell colonies, or confluent monolayers (see above) were rinsed twice with ice-cold Tris-saline. Canine lens plasma membranes from two decapsulated lenses (see above) were washed with Tris-saline and divided into seven equal parts. The aliquots were centrifuged at 16,000 *g* for 10 min and the supernatant was discarded. All subsequent operations were performed at 0–4°C. Cells and lens membranes were incubated for 30 min on ice in the following solutions: (*a*) 0.1 N NaOH; (*b*) 0.1 mM Tris-HCl, pH 7.5, 0.1 mM EGTA, 0.1 mM EDTA, 1 mM PMSF; (*c*) 10 mM Tris-HCl, pH 7.5, 5 mM EGTA, 5 mM EDTA, 1 mM PMSF (Buffer A) containing 6 M urea; (*d*) Buffer A containing 25 mM KCl, 120 mM NaCl, 0.1 mM DTT, 0.5% (vol/vol) Triton X-100; (*e*) Buffer A containing 1 M KCl, 0.1 mM DTT, 0.5% (vol/vol) Triton X-100; and (*f*) Buffer A containing 2 mM diamide, 0.5% (vol/vol) Triton X-100 (two aliquots). Subsequently, the diamide-treated insoluble material was extracted for 30 min on ice with Buffer A containing 6 M urea in the presence or absence of 20 mM DTT. Cells were incubated in petri dishes on a rocking platform, and the lens membranes were vortexed occasionally. At the end of the incubation period, the cells were scraped from the petri dishes in extraction buffer with a rubber policeman. All samples were centrifuged at 16,000 *g* for 10 min. The resulting supernatants were dialyzed against Buffer A and lyophilized; supernatants containing Triton X-100 were first incubated with SM-2 Biobeads (Bio-Rad Laboratories, Richmond, CA) for 2 h at 4°C. Lyophilized supernatants and the extraction residues were solubilized by boiling for 3 min in equal volumes of SDS sample buffer, and analyzed by SDS PAGE followed by immunoblotting with specific antisera.

Immunofluorescence

MDCK cells were grown on collagen-coated glass coverslips. For indirect immunofluorescence microscopy, the cells were rinsed in PBS and processed as follows.

Apical Surface Staining (Confluent Monolayers Only). Cells were fixed with 1.75% (wt/vol) formaldehyde in PBS for 10 min at room temperature. The tight junctions that surround the apical surface prevent antibodies from reaching the basolateral surface (74).

Apical and Basolateral Surface Staining. Cells were incubated for 2–5 min at 37°C in a buffer containing 2 mM EGTA in PBS, and then fixed with 1.75% (wt/vol) formaldehyde in PBS. Under these conditions, the tight junctions are separated and the basolateral surface is accessible to the antibodies (74).

Intracellular Staining. Cells were fixed with 1.75% (wt/vol) formaldehyde in PBS, washed in PBS for 10 min, and then permeabilized with PBS containing 0.5% (vol/vol) Triton X-100, 2 mM $MgCl_2$ for 2–15 min at room temperature. Subsequently, all samples were treated identically. Cells were incubated in a 1:10–1:100 dilution of preimmune or specific antisera in PBS for 30 min at 37°C in a humidified atmosphere. The cells were washed extensively with PBS, and then incubated in a 1:150 dilution of affinity-purified goat anti-rabbit IgG conjugated with rhodamine (Boehringer Mannheim Biochemicals, Indianapolis, IN) in PBS for 30 min at 37°C in a humidified atmosphere. After extensive washing in PBS, coverslips were mounted in Elvanol (80) and viewed with a 63× objective using a Zeiss Universal Microscope equipped with epifluorescence illumination, and photographed on Tri-X Pan film.

Electron Microscopy

MDCK cells were grown on collagen- and carbon-coated coverslips. Cells were fixed in a solution containing 1.25% glutaraldehyde, 1% OsO_4 in 50 mM Pipes, pH 7.2, for 5 min at room temperature. The cells were washed twice in 50 mM Pipes, pH 7.2 (5 min each), and dehydrated sequentially for 5 min each in 60% ethanol; 2% uranyl acetate in 60% ethanol; 80% ethanol; twice in 95% ethanol; five times in 100% ethanol; twice in 100% propylene oxide. The cells were embedded in Epon-Araldite. Silver sections were cut using an LKB ultramicrotome (LKB Instruments, Inc., Gaithersburg, MD), stained in uranyl acetate/lead citrate, and viewed in a Philips 420 transmission electron microscope operated at 80 kV.

Results

Morphology of MDCK Cells in Cultures of Single Cells, Small Colonies, and Confluent Monolayers

MDCK cells were analyzed at three stages during the development of a continuous monolayer culture by phase-contrast and transmission electron microscopy. These stages, single-cell (Fig. 1, *A* and *B*), small colony (Fig. 1, *C* and *D*), and confluent monolayer (Fig. 1, *E* and *F*), represent the cultures used for subsequent analysis of fodrin organization by metabolic labeling, immunofluorescence, and immunoblotting (see below).

Single MDCK cells (Fig. 1, *A* and *B*) exhibit little or no membrane differentiation with the exception of a few microvilli on the apical surface. Cells comprising small colonies (<50 cells) are relatively flat in profile (Fig. 1, *C–E*) compared to cells in a continuous monolayer. The cells exhibit zonula occludens and a few desmosomes. However, there is not extensive cell–cell contact (Fig. 1, *D* and *E*, shows an array of four cells). Sections cut in the midline of colonies parallel to the substratum consistently revealed that there is an intercellular space between adjacent cells (data

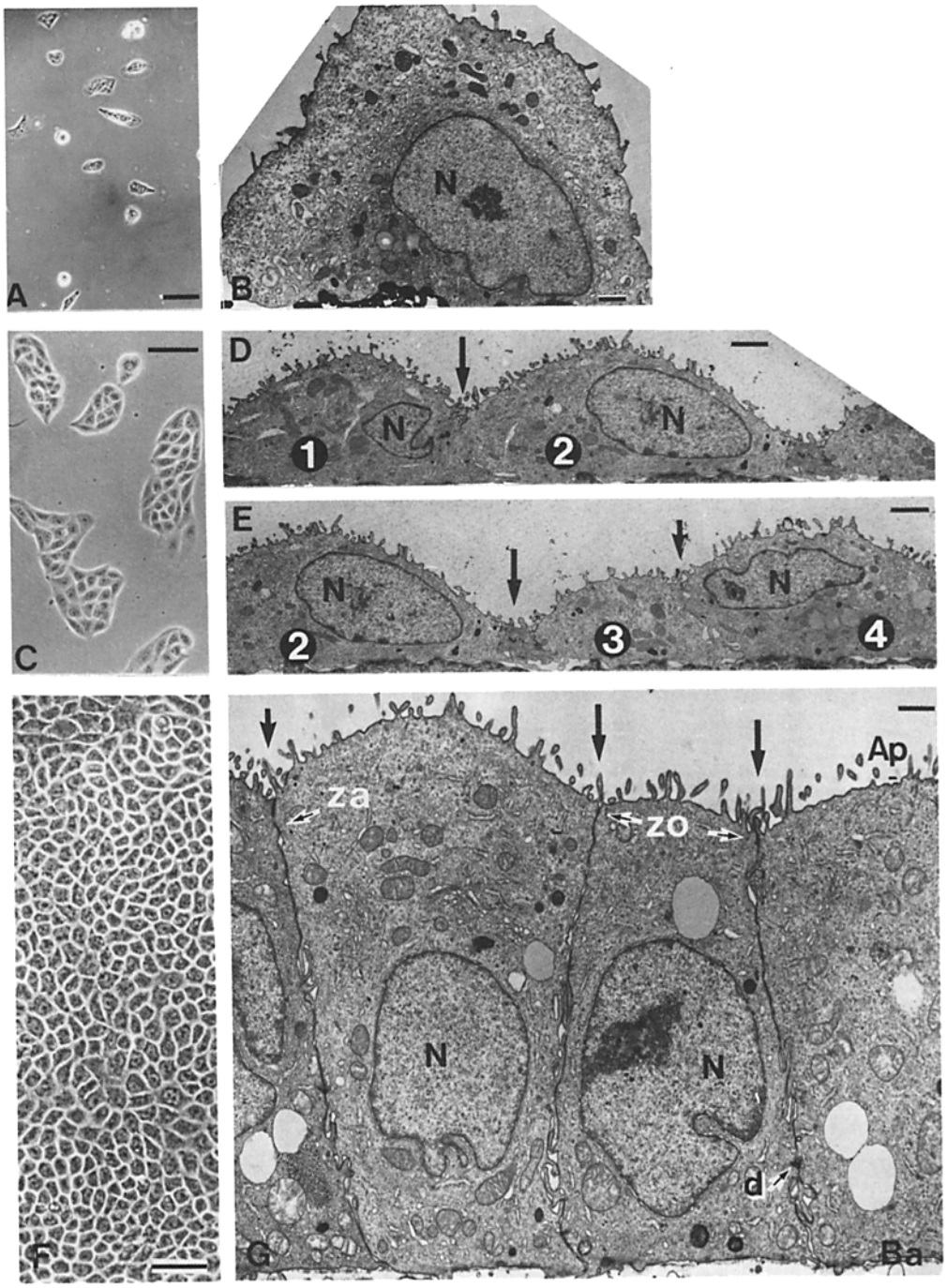

Figure 1. Phase-contrast (*A*, *C*, and *F*) and electron micrographs (*B*, *D*, *E*, and *G*) of MDCK cell cultures during the development of a continuous monolayer. Cells were plated at a density of 1.5×10^4 cells/cm^2 and grown for (*A* and *B*) 12 h, single-cell culture; (*C–E*) 72–96 h, subconfluent culture of MDCK cell colonies (<50 cells/colony); or (*F* and *G*) ~144 h, continuous monolayer of MDCK cells. For electron microscopy cells were sectioned perpendicular to the substratum. *N*, nucleus; *zo*, zonula occludens; *zo*, zonula adherens; *d*, desmosome; *Ap*, apical; *Ba*, basal. Bars, (*A*) 200 μm; (*B*) 1 μm; (*C* and *F*) 100 μm; (*D* and *E*) 2 μm; and (*G*) 0.3 μm.

not shown), indicating that, despite the formation of intercellular junctions, there is not extensive cell–cell contact in small colonies of MDCK cells.

MDCK cells in a continuous monolayer exhibit little or no cell division (Fig. 1 *F*). The cells appear relatively columnal in lateral view, and exhibit a high degree of cell–cell contact and membrane differentiation (Fig. 1 *G*). The lateral membranes exhibit zonula occludens at the boundary of the apical and basolateral membranes, zonula adherans below the zonula occludens, and numerous desmosomes (Fig. 1 *F*). Sections cut parallel to the substratum reveal that the cells are tightly packed together with little evidence of an intercellular space between adjacent cells (data not shown).

Characterization of Antibodies

Previous studies of mammalian and avian lens have shown that fodrin is a major component of isolated membranes. Lens fodrin is composed of two subunits termed α-fodrin (M_r 240,000) and γ-fodrin (M_r 235,000) (28–30, 49, 66) that are structurally and biochemically related to the subunits of the major isoform of fodrin found in brain (6, 29, 30, 50). The α- and γ-subunits of bovine lens fodrin were purified and used as immunogens. Immunoblotting of bovine lens membrane proteins and total MDCK cell proteins revealed that the antisera raised against α-fodrin reacts with a single protein, M_r 240,000 (Figs. 2 *A* [*a*] and 3), and that the antiserum raised against γ-fodrin reacts also with a single polypep-

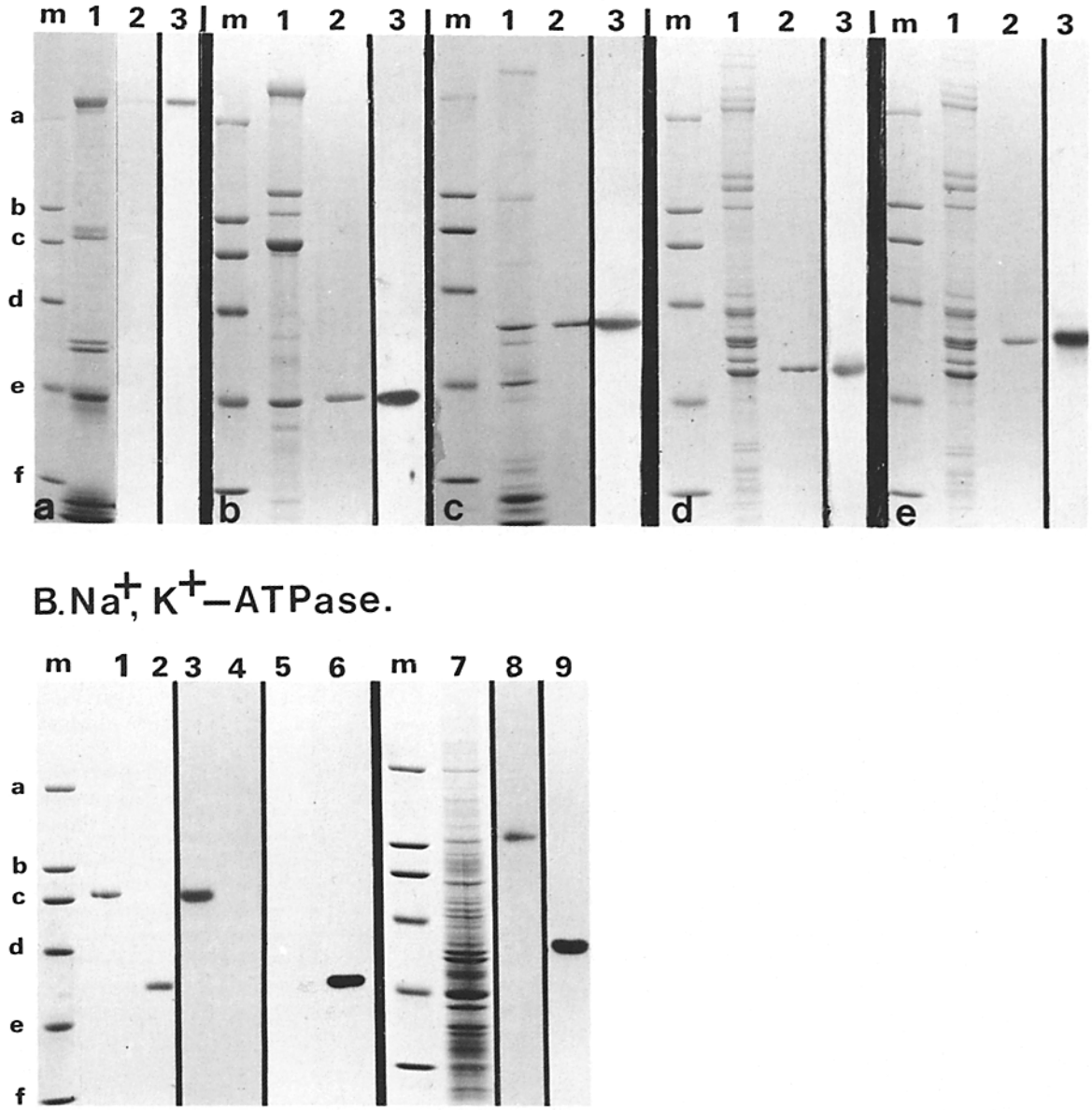

Figure 2. Preparation and characterization of antisera to cytoskeletal proteins (*A*) and the subunits of the Na^+, K^+-ATPase (*B*). (*A*) α-Fodrin (*a*), actin (*b*), vimentin (*c*), and cytokeratins (*d* and *e*) were purified from bovine lens plasma membranes (*a* and *c*, lanes *1*), canine stomach smooth muscle (*b*, lanes *1*), or bovine desmosomes (*d* and *e*, lanes *1*). The purified antigens (lanes *2*) were injected into New Zealand white rabbits. The resulting antiserums to each protein react specifically with the corresponding immunogen in the original tissues (lanes *3*). Lanes *1* and *2* are Coomassie Blue-stained SDS/5–12.5% linear gradient polyacrylamide gels, and lanes *3* are the corresponding autoradiograms of the material in lanes *1* after immunoblotting with antiserum. Lanes *m*, relative molecular mass markers: (*a*) myosin (M_r 205,000); (*b*) β-galactosidase (M_r 116,000); (*c*) phosphorylase b (M_r 97,400); (*d*) bovine albumin (M_r 66,000); (*e*) ovalbumin (M_r 45,000); and (*f*) carbonic anhydrase (M_r 29,000). (*B*) The Na^+, K^+-ATPase was purified from canine kidney by the method described by Jørgensen (36). The α-subunit (M_r 100,000; lane *1*) and β-subunit (M_r ~60,000; lane *2*) were separated and finally purified by SDS PAGE and used as immunogens. The resulting antisera were tested for specificity by immunoblotting; lanes *1* and *2* show a Coomassie Blue-stained gel of the purified subunits and lanes *3–6* are the corresponding autoradiograms after immunoblotting with antiserum to the α-subunit (lanes *3* and *4*) and β-subunit (lanes *5* and *6*). Immunoblotting was also performed on SDS extracts of whole MDCK cells (lane *7*) to show the specificity of the α-(lane *8*) and β-subunit (lane *9*) antisera. Lane *m*, relative molecular mass markers as in *A*.

tide, M_r 235,000 (data not shown; see Fig. 3). High stringency immunoprecipitation of [^{35}S]methionine-labeled proteins from MDCK cells shows that α-fodrin and γ-fodrin are immunoprecipitated specifically with antiserum raised against the corresponding subunit from lens membranes (Fig. 3). However, low stringency immunoprecipitation of [^{35}S]methionine-labeled MDCK proteins solubilized with Triton X-100 shows that an equimolar complex of α- and γ-fodrin is immunoprecipitated with either antisera (Fig. 3, lane *8*, shows the co-immunoprecipitation of α- and γ-fodrin

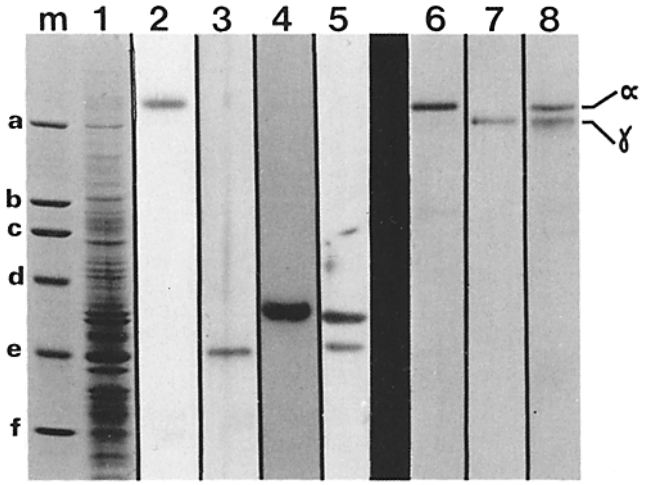

Figure 3. Detection of cytoskeletal proteins in MDCK cells with specific antisera. MDCK cells were lysed in SDS sample buffer and processed for SDS/5–12.5% linear gradient PAGE (lane *1*), and subsequent immunoblotting and autoradiography (lanes *2–5*) with antisera raised against α-fodrin (lane *2*), actin (lane *3*), vimentin (lane *4*), or cytokeratins (lane *5*). Alternatively, MDCK cells were labeled metabolically with [^{35}S]methionine and processed for immunoprecipitation under conditions of high (lanes *6* and *7*) or low (lane *8*) stringency with antisera specific for α-fodrin (lanes *6* and *8*) or γ-fodrin (lane *7*), followed by SDS/5–12.5% linear gradient PAGE and fluorography. Lane *m*, molecular mass markers as in Fig. 2.

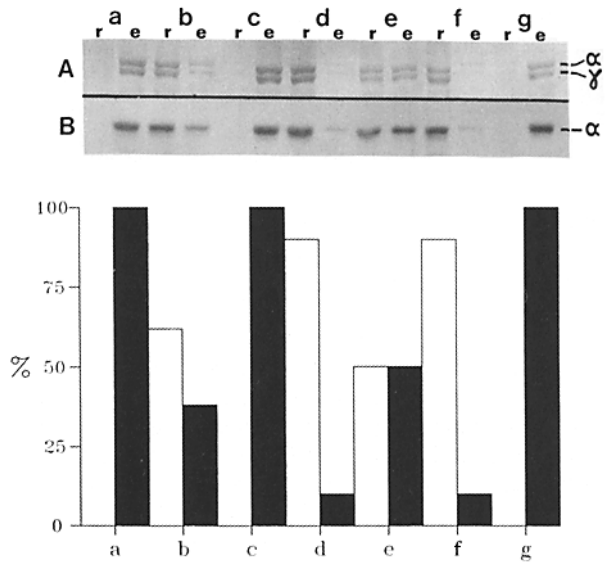

Figure 4. Analysis of the solubility properties of fodrin from canine lens plasma membranes. Lens plasma membranes were prepared as described in Materials and Methods. Fig. 2 A [*a*, lane *1*] shows the starting material for the extraction studies. Equivalent amounts of membranes were treated with different buffers for 30 min at 0°C and then centrifuged to obtain an extract (*e*) and residue (*r*). Membranes were treated with (*a*) 0.1 N NaOH; (*b*) hypotonic Tris/EDTA solution; (*c*) 6 M urea; (*d*) Triton X-100 in 150 mM NaCl/KCl; (*e*) Triton X-100 in 1 M KCl; (*f* and *g*) diamide followed by extraction with 6 M urea under nonreducing (*f*) and reducing (*g*) conditions. The extract and residue of each treatment were subjected to SDS/5% PAGE. The proteins were either stained in the gel with Coomassie Blue (*A*) or transferred to nitrocellulose and processed for immunoblotting with α-fodrin antiserum and autoradiography (*B*). The partitioning of α-fodrin (or γ-fodrin) between the extract and residue after each treatment was determined from densitometric scans of the Coomassie Blue–stained gel (*A*) or the autoradiogram (*B*) or by counting the amount of ^{125}I-protein A bound to the nitrocellulose directly in a γ-counter (data not shown). Each determination gave the same results, and those for α-spectrin are plotted as a histogram (*C*). The relative amounts of α-fodrin in the residue (*white bars*) and extract (*black bars*) are given as a percentage of the original.

with α-fodrin antiserum). The co-immunoprecipitation of α- and γ-fodrin under these conditions may be the result of either the reassociation of subunits during the course of incubation with the antisera, or the immunoprecipitation of a preexisting complex that was solubilized in Triton X-100.

Actin was purified from porcine stomach smooth muscle (Fig. 2 *A* [*b*]). Immunoblotting of the actin-enriched fraction of smooth muscle (24) and MDCK cell proteins shows that the actin antiserum reacts specifically with actin (M_r 42,000) (Figs. 2 and 3).

Vimentin was extracted from bovine lens membranes and purified by single-stranded DNA–cellulose affinity chromatography (Fig. 2 *A* [*c*]). Immunoblotting of lens membrane proteins and MDCK cell proteins shows that the antiserum reacts specifically with vimentin (M_r 58,000) (Figs. 2 and 3).

Cytokeratins were purified from a preparation of bovine desmosomes (Fig. 2 *A* [*d* and *e*]). Antisera were raised against the proteins of M_r 53,000 and M_r 58,000, respectively (Fig. 2, *d* and *e*). Immunoblotting of MDCK cell proteins with a mixture of the antisera revealed reactivity with two proteins M_r 54,000 and M_r 52,000 characterized previously as cytokeratins 8 and 18 (for details, see reference 11) (Figs. 2 and 3).

The Na^+, K^+-ATPase was purified from canine kidney outer medulla as described (36). The purified enzyme is composed of two subunits (α-, M_r 100,000; β-, M_r ~60,000) as shown previously (36). The subunits were purified by SDS PAGE (Fig. 2 *B*, lanes *1* and *2*) and used as immunogens for the preparation of subunit-specific antisera (Fig. 2 *B*, lanes *3–6*). Immunoblotting of an SDS extract of whole MDCK cells (Fig. 2 *B*, lane *7*) shows that the α-subunit antiserum reacts specifically with a polypeptide of apparent M_r 100,000 (Fig. 2 *B*, lane *8*). The antiserum raised against the β-subunit reacts with a relatively diffuse band corresponding to a protein with an apparent M_r ~60,000 (Fig. 2 *B*, lane *9*).

Solubility Properties of Fodrin and Vimentin in MDCK Cells during Development of a Continuous Monolayer: Comparison with Canine Lens Membranes

The solubility properties of fodrin from canine lens membranes was analyzed in order to provide a basis for interpreting the results of fodrin extraction from MDCK cells. Purified lens membranes were subjected to a variety of extraction procedures. The resulting extracts and residues from equivalent amounts of starting material were separated by one-dimensional SDS PAGE (Fig. 4 *A*), and the gels were processed for immunoblotting with α-fodrin antiserum (Fig. 4 *b*); the amount of protein loaded was in the linear range for detection of α-fodrin by immunoblotting (see Fig. 9 *A*). The partitioning of fodrin between the soluble (*e*) and insoluble (*r*) membrane fractions was quantified by three independent methods: (*a*) from densitometric scans of the Coomas-

sie Blue-stained gel; (*b*) from densitometric scans of the autoradiogram; and (*c*) by excising the bands corresponding to α-fodrin from the filter and counting the amount of bound ^{125}I directly in a γ-counter. Each method yielded identical results which are presented in the form of a histogram in Fig. 4 *C*. It should be noted that γ-fodrin has solubility properties identical to those of α-fodrin (see Fig. 4 *A*); the data from the analysis of α-fodrin is presented.

Fodrin is quantitatively extracted from lens membranes with alkaline solutions and high concentrations of urea (Fig. 4, lanes *a* and *c*, respectively). Extraction at 0°C with a buffer of low ionic strength containing divalent cation chelators results in the extraction of ~30% of fodrin (Fig. 4, lane *b*); the relative insolubility of mammalian lens fodrin under these extraction conditions is similar to that of avian erythrocyte spectrin (78) and lens fodrin (66). Extraction of lens membranes with a solution containing 0.5% Triton X-100 and 150 mM salt (NaCl + KCl) results in >90% of the fodrin remaining insoluble (Fig. 4, lane *d*). However, extraction in the presence of 1 M KCl results in the solubilization of ~50% of the fodrin (Fig. 4, lane *e*). To analyze the effect of cross-linking on the extractability of fodrin, lens membranes were treated with 2 mM diamide, a thiol oxidizer, for 30 min at 0°C, and then extracted with 6 M urea in the absence (Fig. 4, lane *f*) or presence of 20 mM DTT (Fig. 4, lane *g*). The results show that pretreatment with diamide causes >90% of the fodrin to remain insoluble in urea, but that the inclusion of the thiol-reducing agent DTT completely reverses this effect.

Cultures of single MDCK cells and continuous monolayers of MDCK cells were extracted with solutions identical to those used above. Cells were extracted on the petri dish in order to maintain the native subcellular distribution and conformation of the protein with respect to cell-substratum and cell-cell contact. After extraction, the residues and extracts were subjected to SDS/5% PAGE and immunoblotting with α-fodrin antiserum. The relative amount of α-fodrin in the soluble and insoluble cell fractions was determined from densitometric scans of the autoradiogram and plotted in the form of histograms (Fig. 5). Fodrin in single cell and confluent monolayer cultures is soluble in solutions of high pH (Fig. 5, *A* and *B*, lane *a*) but relatively resistant to extraction with buffers of low ionic strength (Fig. 5, *A* and *B*, lane *b*). These solubility properties are similar to those of lens fodrin (see Fig. 4). However, in contrast to lens fodrin, 25–35% of fodrin in all types of cultures of MDCK cells is resistant to extraction in the presence of 6 M urea (Fig. 5, *A* and *B*, lane *c*). A significant difference in the solubility properties of fodrin was found between single cells and continuous monolayers upon extraction with solutions containing Triton X-100. In single cells, fodrin is relatively soluble (~50%) in the presence of Triton X-100 and either low or high salt concentrations (Fig. 5 *A*, lanes *d* and *e*, respectively). In contrast, >90% of fodrin in continuous monolayers of cells is insoluble under the same conditions of extraction (Fig. 5 *B*, lanes *d* and *e*). In addition, a significant difference in the extractability of fodrin was detected between single cells and continuous monolayers following oxidative cross-linking; >75% of fodrin in continuous monolayers can be oxidatively cross-linked (Fig. 5 *B*, lane *f*) compared with <35% of fodrin in single cells (Fig. 5 *A*, lane *f*). In both cases, cross-linking can be reversed by inclusion of DTT in the extraction buffer containing urea (Fig. 5, *A* and *B*, lanes *g*).

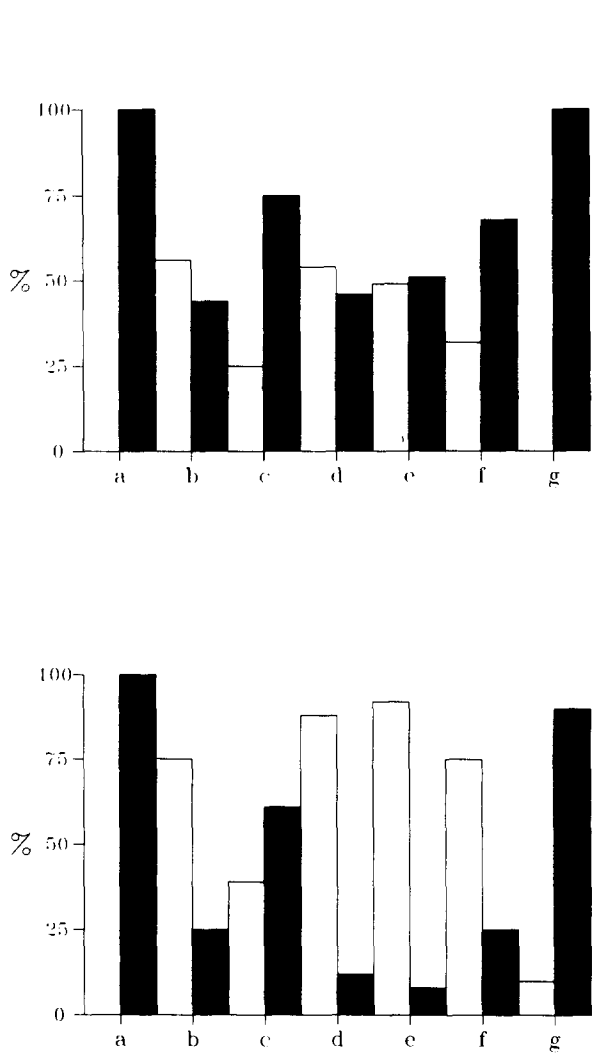

Figure 5. Analysis of the solubility properties of α-fodrin from single-cell (*A*) and confluent monolayer cultures (*B*) of MDCK cells. Replicate cultures of MDCK cells were washed twice with ice-cold Tris-saline and the cells were extracted for 30 min on the petri dish at 4°C in (*a*) 0.1 N NaOH; (*b*) hypotonic Tris/EDTA; (*c*) 6 M urea; (*d*) Triton X-100 and 150 mM NaCl/KCl; (*e*) Triton X-100 and 1 M KCl; and (*f* and *g*) diamide followed by extraction with 6 M urea under nonreducing (*f*) and reducing (*g*) conditions. The cell residues were scraped from the petri dish, centrifuged at 12,000 *g* for 5 min, and the resulting extract and residue were subjected to SDS/5% PAGE and immunoblotting with α-fodrin antiserum. The relative amounts of α-fodrin in each residue (*open bars*) and extract (*solid bars*) were determined from densitometric scans of the resulting autoradiograms and plotted as a histogram.

To provide a control, in addition to lens membranes, we analyzed the extractability of vimentin from different cultures of MDCK cells (Fig. 6, *A* and *B*). In all cases, vimentin is extracted quantitatively with buffers of high pH and high concentrations of urea (Fig. 6, *A* and *B*, lanes *a* and *c*, respectively), but is insoluble in solutions containing Triton X-100 and either low or high salt concentrations (Fig. 6, *A* and *B*, lanes *d* and *e*, respectively). In addition, oxidative cross-linking with diamide has little or no effect on the extractabil-

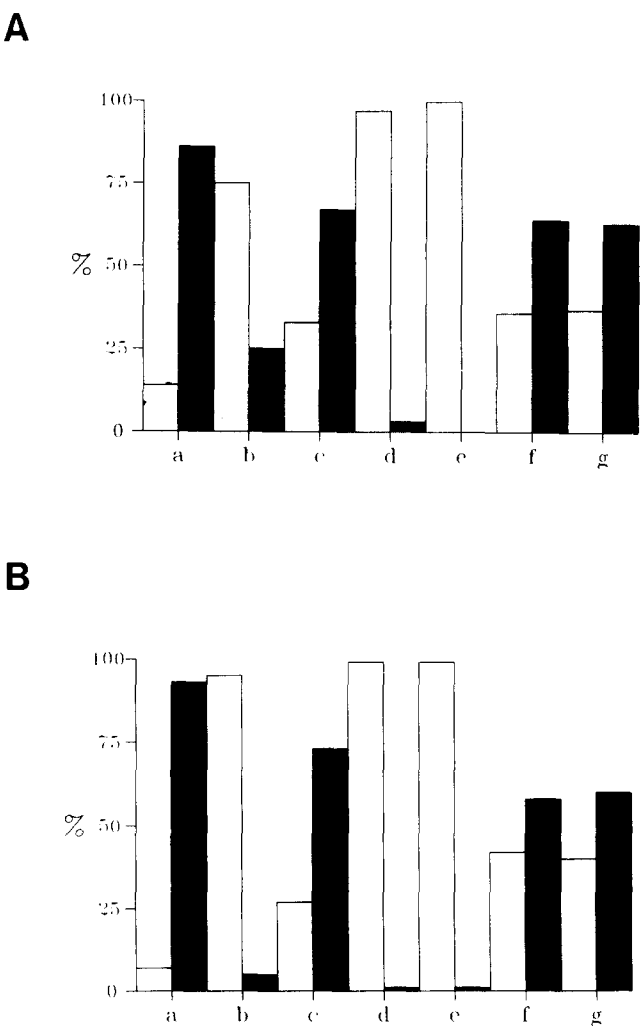

Figure 6. Analysis of the solubility properties of vimentin from single-cell (*A*) and confluent monolayer (*B*) cultures of MDCK cells. Replicate cultures of MDCK cells were extracted and processed for immunoblotting with vimentin antiserum exactly as described in the legend to Fig. 5. The relative amounts of vimentin in each residue (*open bars*) and extract (*solid bars*) were determined from densitometric scans of the resulting autoradiograms and plotted as a histogram.

ity of vimentin with solutions containing 6 M urea (Fig. 6, *A* and *B*, lanes *f* and *g*).

Organization of Fodrin, Actin, and Intermediate Filament Proteins during Development of a Continuous Monolayer of MDCK Cells

The distribution of fodrin, actin, and intermediate filament proteins in single MDCK cells, small colonies of cells, and confluent monolayers of cells (see Fig. 1) was analyzed by indirect immunofluorescence (Fig. 7). Cells were fixed and permeabilized as described previously (64); similar results to those shown here were obtained following fixation and then permeabilization with a range of Triton X-100 concentration (0.1%–1.0%), or following permeabilization and then fixation, or fixation/permeabilization in 100% methanol at −20°C (data not shown).

In single cells, α-fodrin antiserum stains the cytoplasmic surface of the plasma membrane (Fig. 7 *A*). Immunofluorescence with preimmune serum (Fig. 7 *F*) or with antiserum on cells which had not been permeabilized (data not shown) gave little or no staining. Indirect immunofluorescence with α-fodrin antibodies of small colonies of ~10–25 cells revealed extensive staining in the center of each cell similar to that observed in single cells. In addition, however, occasional staining of the membrane in the region of cell–cell contact is apparent (Fig. 7, *B* and *C*). In addition, by focusing on the region of cell–substratum interaction, staining of the basal membrane is apparent (data not shown). At the time when individual colonies begin to coalesce to form a continuous monolayer (~day 5 after plating single cells), there is a dramatic change in the subcellular distribution of spectrin. The cells no longer exhibit uniform staining of the membrane, but instead show intense staining at the periphery of adjacent cells (Fig. 7, *D* and *E*). Focusing on the apical surfaces of the monolayer reveals staining of the cell periphery but relatively little or no staining at the center of the cells at the plane of the apical membranes (Fig. 7 *D*). However, analysis at a focal plane close to the substratum (Fig. 7 *E*) reveals staining at both the cell periphery and in the center of the cells. This asymmetric distribution of α-fodrin is maintained in continuous monolayers of MDCK cells that have been confluent for 7 d (data not shown). Immunofluorescence analysis of confluent monolayers of MDCK cells with γ-fodrin antisera revealed a distribution of this subunit similar to that of α-fodrin (data not shown).

Indirect immunofluorescence with actin antiserum was also performed on MDCK cells during development of a continuous monolayer (Fig. 7, *G–K*). In single cells, stress fibers are stained intensely with the actin antiserum (Fig. 7 *G*). The stress fibers traverse the cell from end-to-end and are present, to a lesser degree, at the cell boundary (Fig. 7 *G*). Analysis of pairs of MDCK cells (presumably daughter cells; Fig. 7 *h'*) and small colonies of cells (Fig. 7, *H* and *I*) revealed an intense staining of the lateral membranes of adjacent cells; the stained material did not appear to be composed of stress fibers. In continuous monolayers of MDCK cells, actin staining is almost exclusively limited to the lateral membrane (Fig. 7 *J*). Few stress fibers are observed. The overall speckled staining in the center of each cell appears to be localized to the apical membrane and, presumably, to the numerous microvilli (Fig. 1).

In contrast to the dramatic changes in the subcellular distribution of fodrin and actin observed during the development of a continuous monolayer of MDCK cells, immunofluorescence with antisera to vimentin (Fig. 7, *L–P*) and cytokeratins (Fig. 7, *Q–T*) revealed little or no change in the distribution of these intermediate filament proteins. Single cells, small colonies of cells, and cells in continuous monolayers exhibit a similar cytoplasmic distribution of vimentin filaments. In particular, vimentin filaments are not organized close to the plasma membrane in single cells (Fig. 7 *L*), or in cells which exhibit extensive cell–cell contact (Fig. 7, *N* and *O*). Immunofluorescence with cytokeratin antisera revealed a distribution of this intermediate filament network that is more closely associated with the plasma membrane than that of vimentin. This association is evident in small colonies of cells in which desmosomes are present (Fig. 7 *R*; Fig. 1), and does not change significantly during the formation of a continuous monolayer of cells (Fig. 7 *S*).

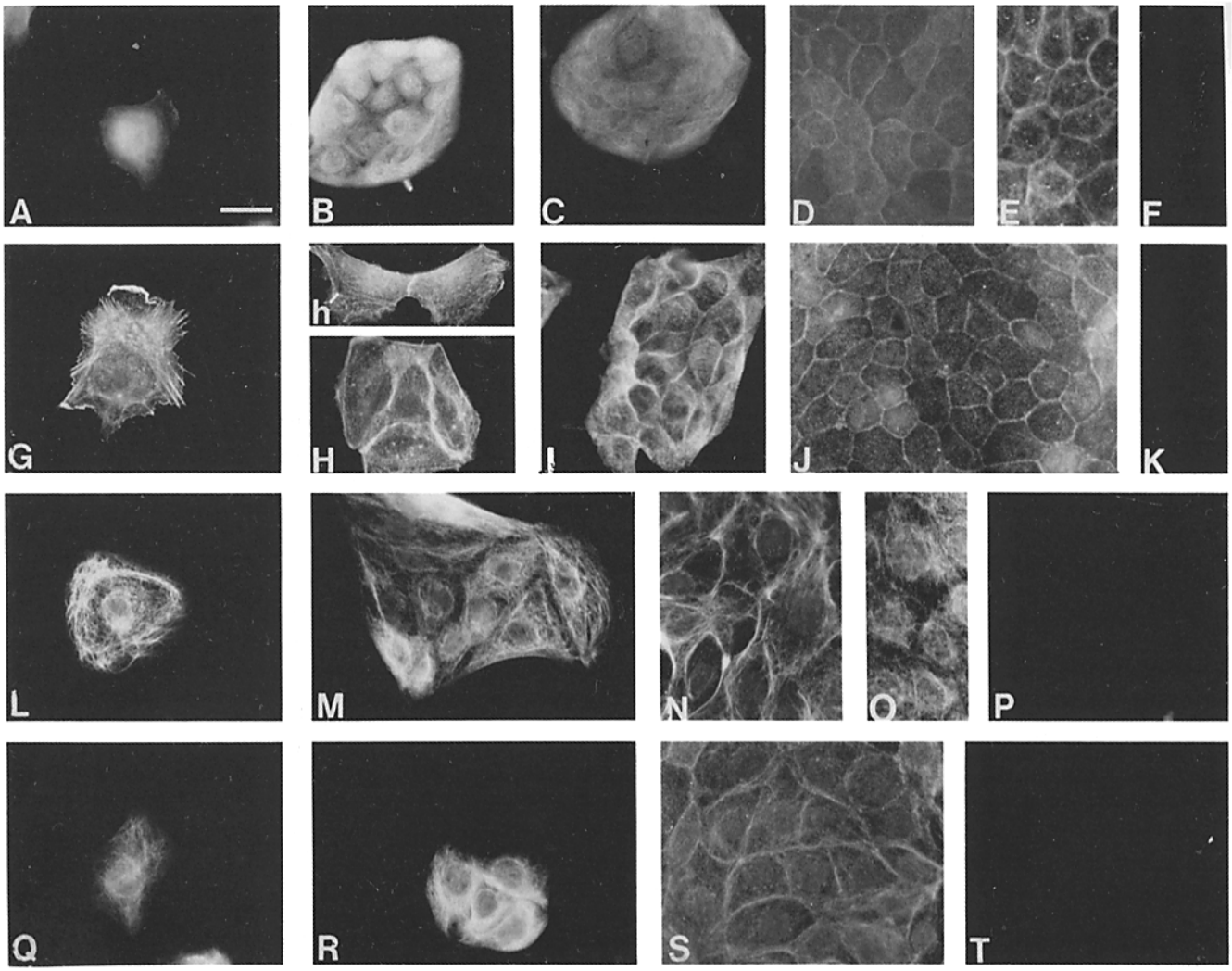

Figure 7. Indirect immunofluorescence of cytoskeletal proteins in MDCK cells during development of a continuous monolayer. Single-cell (*A*, *G*, *L*, and *Q*), small colony (*B*, *C*, *h'*, *H*, *I*, *M*, and *R*), and confluent monolayer (*D*, *E*, *J*, *N*, *O*, and *S*) cultures of MDCK cells were grown on collagen-coated glass coverslips and fixed with 1.75% formaldehyde and then permeabilized in 0.5% vol/vol Triton X-100. The cells were processed for indirect immunofluorescence with antisera specific for α-fodrin (*A–E*), actin (*G–J*), vimentin (*L–O*), or cytokeratins (*Q–S*), or preimmune serum (*F*, α-fodrin; *K*, actin; *P*, vimentin; *T*, cytokeratins), followed by affinity-purified, rhodamine-labeled goat anti-rabbit IgG. Antisera were diluted 1:10 (cytokeratin, α-fodrin) or 1:100 (actin, vimentin). Coverslips were mounted in Elvanol, and the cells viewed in a Zeiss Universal Microscope equipped for epifluorescence. Bar, 20 μm.

Turnover of Newly Synthesized Fodrin during Development of a Continuous Monolayer of MDCK Cells

To analyze the stability of newly synthesized fodrin during development of a continuous monolayer, cultures of MDCK cells at different densities were pulse-labeled with [^{35}S]methionine for 15 min, and then incubated for up to 17 h in a >10,000-fold excess of unlabeled methionine (chase period). Newly synthesized α- and γ-fodrin were detected by immunoprecipitation and fluorography (see Fig. 3, lanes *6* and *7*). The relative amounts of [^{35}S]methionine-labeled fodrin subunits, after different periods of chase, were determined by scanning densitometry, and the results were subjected to regression analysis to determine the half-lives. The half-lives calculated for the fodrin subunits represent the range between three independent experiments. Fig. 8 shows the analysis of α-fodrin from one of these experiments; similar results were obtained for γ-fodrin (data not shown). A dramatic difference in the stability of newly synthesized fodrin subunits was found between single cells and cells in a continuous monolayer. In single cells, the half-lives of α- and γ-fodrin were calculated to be 12–16 h. In subconfluent cultures of cells, comprising colonies of 50–100 cells (day 4), the half-lives of the fodrin subunits were ~30–36 h. However, in cultures of MDCK cells that had just become confluent (day 6), the half-lives of the fodrin subunits were calculated to be >70 h.

Accumulation of Fodrin at Steady State during Development of a Continuous Monolayer of MDCK Cells

The results described above demonstrate a dramatic decrease in the rate of turnover of newly synthesized fodrin during growth of MDCK cell cultures from single cells to confluent

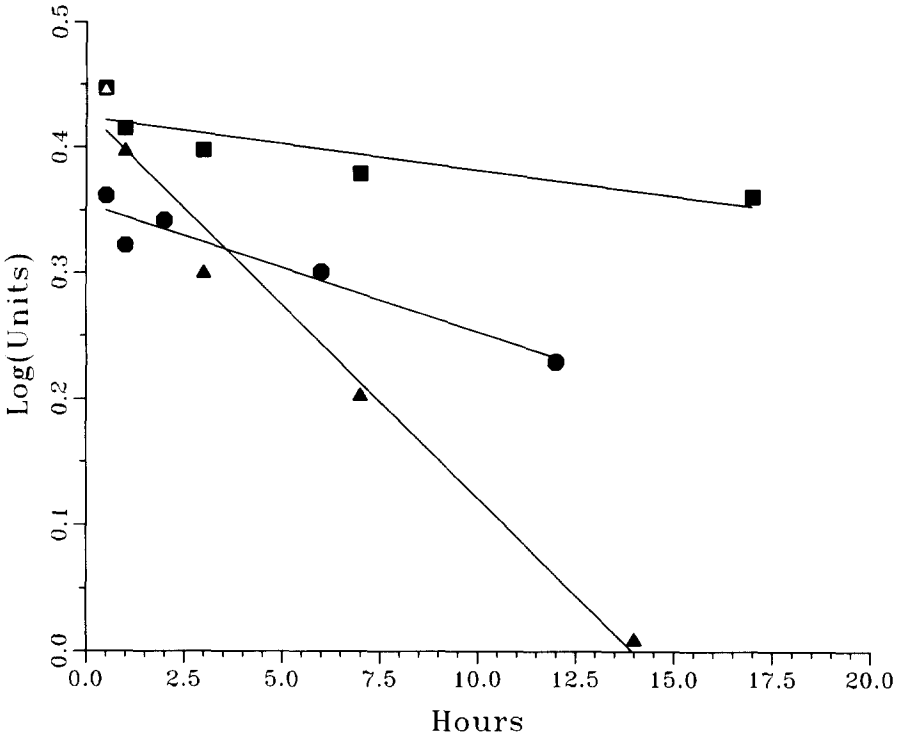

Figure 8. Turnover of newly synthesized α-fodrin in MDCK cells in cultures of different cell density. Single-cell (△), <75-cell colony (●), and confluent monolayer (■) cultures of MDCK cells were metabolically labeled with [^{35}S]methionine for 15 min at 37°C (pulse) and then incubated in >10,000-fold excess of unlabeled methionine for different periods of time (chase). Cells were scraped from the petri dish and processed for immunoprecipitation with α-fodrin antiserum, followed by SDS PAGE and fluorography. The relative amount of [^{35}S]methionine-labeled α-fodrin was determined from densitometric scans of the resulting fluorograms and plotted against the time of chase using regression analysis; the rate of turnover of newly synthesized α-fodrin was calculated by regression analysis.

monolayers of cells. To determine whether this increasing stability of fodrin is reflected in changes in the steady-state level of the protein, MDCK cells were analyzed by immunoblotting with α-fodrin antiserum during the formation of a continuous monolayer; the amount of protein analyzed at each stage in the growth of replicate cultures was normalized to the DNA concentration. Fig. 9 *A* shows that the amount of protein analyzed was within the linear range for quantitation of α-fodrin by immunoblotting. The analysis by immunoblotting was standardized with different amounts of total MDCK protein, rather than with pure fodrin, to ensure that the detection of fodrin was within the linear range in a complex mixture of proteins that would be used for the analysis of fodrin levels in MDCK cells during the development of a continuous monolayer.

The analysis of the steady-state levels of fodrin revealed a dramatic accumulation of fodrin during the growth of MDCK cell cultures (Fig. 9 *B*). The rate of fodrin accumulation, however, does not appear to be constant during the development of a continuous monolayer. Instead, the period of accumulation is limited to the time between days 3–7 when individual colonies of MDCK cells coalesce to form a continuous monolayer (see Fig. 1). Rapidly dividing cells (days 1–3) exhibit relatively constant steady-state levels of fodrin. Similarly, cells in a continuous monolayer (day 7 onwards) exhibit little or no change in the amount of fodrin accumulated between days 3 and 7.

Development of Polarity in the Distribution of the Na$^+$, K$^+$-ATPase in Cultures of MDCK Cells

Indirect immunofluorescence was performed on MDCK cells at different stages of development of a continuous monolayer; a combination of α- and β-subunit-specific antisera was used (Fig. 10). Single MDCK cells exhibit a uniform staining of the membrane either after fixation and permeabilization (Fig. 10 *A*) or fixation alone (data not shown). Immunofluorescence of small colonies of cells (4–20 cells) also revealed a predominantly uniform staining of the plasma membrane with antisera to the Na$^+$, K$^+$-ATPase subunits (Fig. 10 *B*). Occasionally, however, the lateral membranes of adjacent cells exhibited intense staining (Fig. 10 *B*). The proportion of cells exhibiting staining of the lateral membranes increased dramatically upon formation of a continuous monolayer. Monolayers of cells that had been processed for basolateral and apical surface staining or intracellular/surface staining (see Materials and Methods) showed an almost exclusive localization of the Na$^+$, K$^+$-ATPase to the basolateral surface, and particularly the lateral membrane (Fig. 10, *F* and *G*). Cells that had been processed for apical surface staining (see Materials and Methods) exhibit little or no fluorescence with Na$^+$, K$^+$-ATPase subunit antisera (Fig. 10 *E*), similar to that obtained with the preimmune serum (Fig. 10 *D*). Thus, these results demonstrate that the formation of a continuous monolayer of MDCK cells coincides with the development in the polarized organization of the Na$^+$, K$^+$-ATPase onto the basolateral membrane.

Discussion

The differentiation of the plasma membrane into functionally and structurally distinct domains is characteristic of cells which exhibit a polarized organization. At present, the mechanisms regulating the formation of membrane domains are poorly understood. Clearly, there are two fundamental aspects of this problem; first, newly synthesized membrane proteins must be directed to the correct domain of the membrane; and second, upon arrival at the correct membrane, the lateral mobility of proteins must be restricted in order to maintain the functional and structural specificity of the membrane domain. Recent studies of the budding of enveloped

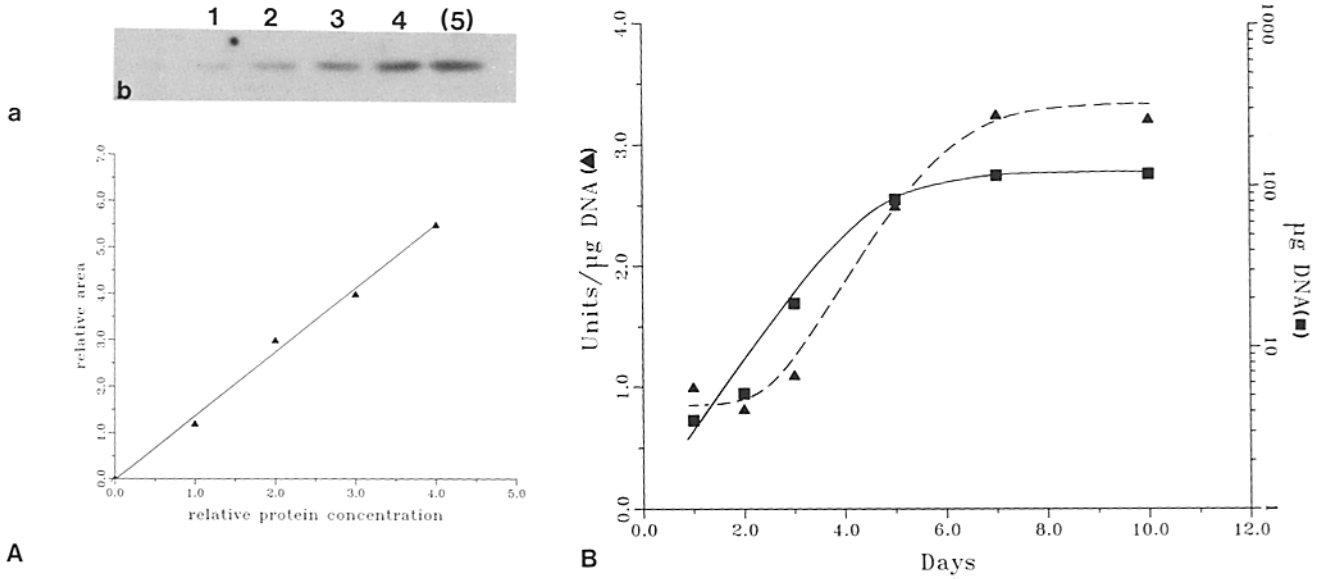

Figure 9. Steady-state levels of fodrin in cultures of MDCK cells. (*A*) Detection of different amounts of α-fodrin in extracts of MDCK cells by immunoblotting. MDCK cells were lysed in SDS sample buffer and different amounts of protein over a fivefold concentration range were applied to an SDS/5% polyacrylamide gel. After immunoblotting with α-fodrin antibodies, the relative amount of α-fodrin was determined by densitometric scans of the autoradiogram (*a*) and the relative area under each peak was plotted against the relative protein concentration (*b*). Under these conditions, the amount of α-fodrin in complex mixtures of proteins was in the linear range for detection by immunoblotting. (*B*) Analysis of the steady-state levels of α-fodrin in MDCK cells during development of a continuous monolayer. Replicate cultures of MDCK cells were plated at an initial density of 1.5×10^4 cells/cm^2. On days 1, 2, 3, 5, 7, and 10, cultures of cells were processed for SDS PAGE and immunoblotting with α-fodrin antiserum. The relative amount of α-fodrin was normalized to the DNA concentration of the petri dish, and was in the linear range for detection of α-fodrin by immunoblotting. The relative amount of α-fodrin was determined from densitometric scans of the resulting autoradiograms. The amount of DNA was determined by the method described by Labarca and Paigen (42).

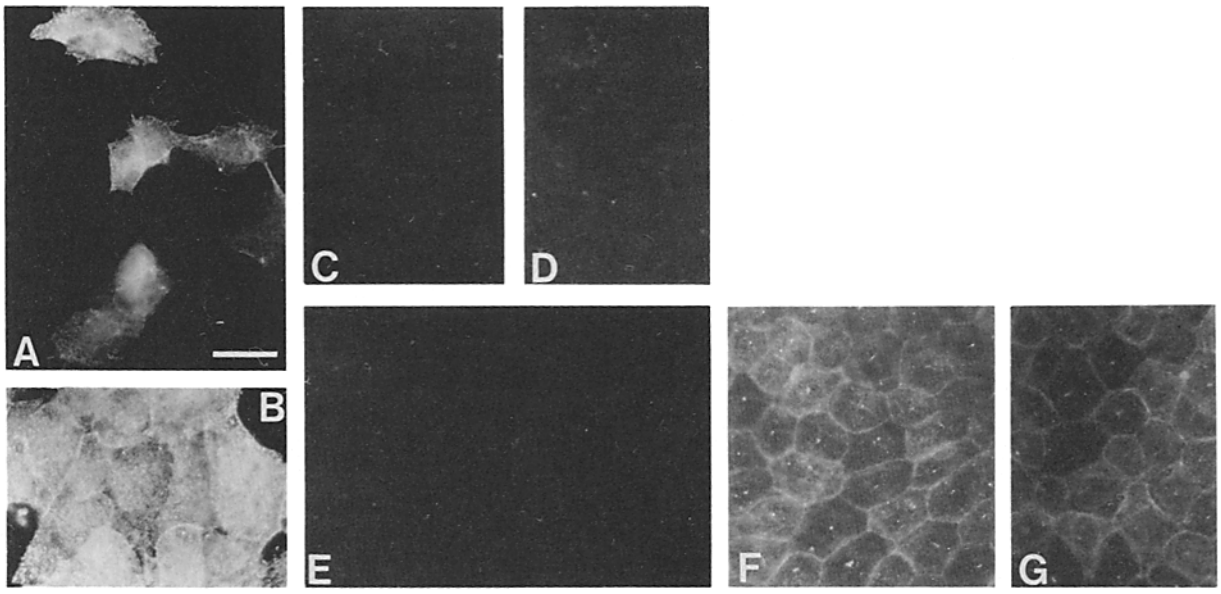

Figure 10. Indirect immunofluorescence of the Na^+, K^+-ATPase in MDCK cells during the development of a continuous monolayer. Single-cell (*A*), <50-cell colony (*B*), and confluent monolayer (*C–G*) cultures of MDCK cells were grown on collagen-coated glass coverslips. The cells were fixed with 1.75% formaldehyde and either first permeabilized with Triton X-100 and then processed (*A–C*, *F*, and *G*), or processed directly with a 1:10 dilution of α- and β-subunit antisera (*E*), or preimmune serum (*D*) followed by affinity-purified, rhodamine-labeled goat anti-rabbit IgG. The cells were viewed in a Zeiss Universal Microscope equipped for epifluorescence. Bar, 20 μm.

RNA viruses from polarized MDCK cells have resulted in significant advances in our understanding of the pathways of protein targeting to different membrane domains (reviewed in references 81 and 86). Studies on the topogenesis of the envelope glycoproteins of influenza virus and vesicular stomatitis virus have shown that these proteins are sorted intracellularly and targeted directly either to the apical (hemagglutinin; influenza virus) or basolateral (G protein; vesicular stomatitis virus) domains of the plasma membrane (56, 60, 75, 79). By comparison, little is known about the mechanism(s) involved in maintaining the asymmetric distribution of membrane proteins in these polarized cells. To address this important aspect of the regulation of membrane differentiation, we have sought to analyze the role of the membrane skeleton. In this study we have identified and characterized fodrin in MDCK cells, with the perspective that this protein, as in erythrocytes, may play an important role in membrane protein organization.

Analysis of total MDCK proteins by immunoblotting or high stringency immunoprecipitation with subunit-specific lens fodrin antisera revealed the presence of two immunologically distinct subunits, M_r 240,000 and M_r 235,000; these relative molecular masses are similar to those of α- and γ-fodrin, respectively, determined previously in lens (49, 66) and brain (6, 46, 50; see also references 29 and 30). The M_r 240,000 subunit reacted specifically with antiserum raised against lens α-fodrin, while the M_r 235,000 subunit reacted specifically with antiserum raised against lens γ-fodrin. That these subunits form a complex was demonstrated by the fact that low stringency immunoprecipitation of [^{35}S]methionine-labeled proteins from MDCK cells with α- or γ-fodrin antiserum resulted in the isolation of a complex of these two subunits in a 1:1 molar ratio (Fig. 2 and 3). This confirms previous studies which have shown that α- and γ-fodrin can be co-immunoprecipitated as an equimolar complex from extracts of myoblasts (64), lens (66), and neurons (47). Together these results demonstrate that MDCK cells express an isoform of fodrin which has a subunit composition and stoichiometry similar to that of fodrin characterized previously from lens. We are currently purifying kidney fodrin to compare the physiochemical properties of kidney, lens, and brain fodrin directly.

Mammalian (αβ-) spectrin can be selectively extracted from erythrocyte plasma membranes by treatment with alkaline solutions (87), low ionic strength solution containing EDTA (54), and high concentrations of urea (38). To characterize the solubility properties of mammalian αγ-fodrin, we analyzed fodrin from lens fiber cell membranes (Fig. 4). Our results showed that lens fodrin has solubility properties similar to those of erythrocyte spectrin, with the exception that αγ-fodrin was less readily extracted with buffers of low ionic strength (Fig. 4); this confirms the results of a previous comparative study of the solubility properties of avian erythrocyte spectrin and lens fodrin (66). These results provided a basis for analyzing the solubility properties of αγ-fodrin from MDCK cells (Fig. 5). The results showed that fodrin in a continuous monolayer has solubility properties similar to those of lens fodrin, whereas fodrin in single cells was more easily solubilized. In single cells, fodrin was relatively soluble in solutions containing Triton X-100 and either high or low salt concentrations, and in solutions containing 6 M urea after attempts to oxidatively cross-link the protein with diamide. However, fodrin in continuous monolayers of MDCK cells was almost completely insoluble under the same extraction conditions.

There are several possible explanations of the differences between the solubility properties of fodrin from single MDCK cells and confluent monolayers of cells. A trivial explanation is that the extraction buffers were unable to penetrate and equilibrate within confluent monolayers of cells as efficiently as within single cells. However, identical results to those presented here were obtained using different volumes of buffer (up to 5 ml; data not shown) and times of incubation (10–60 min; data not shown). Furthermore, the solubility properties of vimentin, a cytoplasmic filament protein, were shown to be identical in single and confluent monolayers of cells (Fig. 6). Thus, these results indicate that the extraction buffers were able to equilibrate to the same degree within MDCK cells in single-cell and confluent cultures.

Alternatively, these differences may be due to a change in the disposition of fodrin on the membrane that occurs during the development of a continuous monolayer of MDCK cells. A change consistent with the dramatic increase in the insolubility of fodrin is the gradual formation of a dense meshwork of fodrin which is attached to the plasma membrane of MDCK cells, similar to that of the spectrin-based membrane skeleton of the erythrocyte. The formation of this protein meshwork on the membrane could be brought about by the reorganization and concentration of fodrin into a localized region of the membrane, or by the gradual accumulation of newly synthesized fodrin at steady state. Our analyses of the distribution and steady-state levels of fodrin indicate that both of these processes occur during the development of a continuous monolayer of MDCK cells.

Indirect immunofluorescence revealed that the distribution of fodrin appeared to undergo a dramatic change during development of a continuous monolayer of MDCK cells, from a random distribution on the plasma membrane of single cells to an apparent asymmetric distribution at the periphery of cells in regions of extensive cell–cell contact in continuous monolayers (Fig. 7). Although our analysis of fodrin distribution in the *en face* view in cells in a continuous monolayer is subject to interpretation, we were able to analyze the distribution of fodrin at different focal planes due to the relative columnal form of MDCK cells in confluent monolayers (see Fig. 1 *F*). Analysis at the apical surface (Fig. 7 *D*) revealed a ring of fodrin around each cell in association with the lateral membrane, but little or no staining in the center of the cell at the level of the apical plasma membrane. Analysis of fodrin fluorescence at the basal surface (Fig. 7 *E*) also revealed intense staining at the lateral membranes and, in addition, staining at the level of the basal plasma membrane. We interpret this staining pattern as evidence of a fodrin distribution that is predominantly basolateral, although we cannot rule out the possibility at present that a small fraction of fodrin remains associated with the apical membrane.

It may be significant that the appearance of this asymmetric distribution of fodrin was not induced immediately upon cell contact, since we found that colonies of up to ~40 cells exhibited little or no staining of the lateral membranes, compared with that in the cells in confluent monolayers (Fig. 7, *A–D*). This is in contrast to actin, which was localized predominantly to the lateral membranes of adjacent cells in

all sizes of cell colonies (Fig. 7, *G–K*; see also references 39 and 59). The change in fodrin distribution also contrasted with the distributions of intermediate filament proteins (vimentin and cytokeratin; Fig. 7, *L–P*, and *Q–T*, respectively) and tubulin (data not shown) which underwent little or no change during the development of a continuous monolayer of cells (see also reference 11). These results indicate that the regulation of fodrin distribution on the membrane of MDCK cells is not coupled to that of actin, tubulin, or intermediate filament proteins. Thus, it appears that these proteins, at least initially, may play different roles in cell organization during the development of a continuous monolayer of MDCK cells. For instance, actin is a component of the zonula adherens, a junctional complex localized to the lateral membranes of adjacent cells which is involved in establishing cell–cell contact (reviewed in reference 26); and cytokeratin-containing intermediate filaments are thought to be involved in the organization of desmosomes (12, 35, 71).

That fodrin accumulates at steady state during development of a continuous monolayer was demonstrated by immunoblotting (Fig. 9). An approximately fivefold increase, normalized to the DNA concentration of each petri dish, was detected. This increase occurred between days 3 and 7 of the growth of the cell culture. Rapidly dividing cells (days 1 and 3) and continuous monolayers of MDCK cells (>day 6) did not accumulate fodrin. The molecular basis for these differences in the rates of fodrin accumulation was provided by an analysis of the rate of turnover of newly synthesized fodrin (Fig. 8). In single MDCK cells, which double in ~16 h (see Fig. 9), newly synthesized fodrin was degraded with an apparent $t_{1/2}$ of 12–16 h; as a consequence fodrin would not be expected to accumulate at steady state, as demonstrated by immunoblotting. However, the rate of turnover of newly synthesized fodrin in subconfluent cultures (day 4) is dramatically decreased ($t_{1/2} > 30$ h) at a time when the amount of fodrin at steady state began to increase as detected by immunoblotting. Analysis of the rate of turnover of newly synthesized fodrin in a continuous monolayer of MDCK cells revealed a $t_{1/2}$ of >70 h. The relatively long half-life of fodrin in confluent cultures of MDCK cells, combined with a decline in the rate of fodrin synthesis upon formation of a continuous monolayer (data not shown), would be expected to result in the maintenance of levels of fodrin at steady state that were reached at the end of the period of fodrin accumulation, as demonstrated also by immunoblotting.

Taken together, these results strongly indicate a temporal and spatial relationship between the development of a continuous monolayer of MDCK cells and the increased insolubility, decreased turnover and concomitant accumulation, and redistribution of fodrin in these cells. We interpret these changes as evidence for the gradual formation of an insoluble, relatively dense and stable meshwork of fodrin that appears to be predominantly localized to the cytoplasmic surface of the basolateral plasma membrane domain in regions of extensive cell–cell contact of MDCK cells. What could be the function of this structure? At present, we have no direct evidence that fodrin is linked to integral membrane proteins, and hence plays a role in maintaining membrane domains. However, the solubility properties of fodrin in a continuous monolayer of MDCK cells are similar to those of spectrin in erythrocytes in which this linkage has been firmly established (reviewed in references 5, 15, and 20). Furthermore, it may be significant that the formation of this structure coincides with the development of the polarized distribution of the Na^+, K^+-ATPase, a marker protein of the basolateral domain of the plasma membrane (Fig. 10).

Analysis by immunofluorescence of the distribution of the Na^+, K^+-ATPase in a continuous monolayer of MDCK cells revealed an asymmetric distribution of the enzyme on the basolateral membrane (see also references 40, 41, 44, and 52). This polarized distribution of the Na^+, K^+-ATPase is functionally significant in cells of transporting epithelia in which the Na^+ fluxes generated by the enzyme across the cell drive the transcellular movement of ions and metabolites from the apical to the basolateral surfaces (reviewed in references 27 and 37). The development of cell surface polarity of the Na^+, K^+-ATPase was shown to be gradual during the growth of MDCK cultures, as has been shown recently for other basolateral membrane proteins (4, 33), and coincided temporally and spatially with changes in the distribution of fodrin, but not with the distribution of actin, intermediate filaments, or microtubules.

That the development of cell surface polarity of the Na^+, K^+-ATPase and the reorganization of fodrin occurred in nearly confluent cultures of MDCK cells and not in small colonies of cells indicates that extensive cell–cell contact plays an important role in the development of the asymmetric distributions of these proteins. Indeed, our analysis by electron microscopy showed a clear difference in the degree of cell–cell contact between cells in small colonies and confluent monolayers (Fig. 1). The significance of cell–cell contact in membrane differentiation of polarized epithelial cells has been noted previously, although in these cases emphasis was placed on the formation of the zonula occludens and the role of this junctional complex as a physical barrier to the lateral diffusion of proteins between the apical and basolateral domains of the membrane (25, 31, 52, 57, 72, 76, 84). However, it may be significant that perturbations to the external surface of the membrane of erythroid (23, 28, 38, 85) and nonerythroid (14, 48, 51, 69, 73, 77) cells have been shown to have a dramatic effect on the distribution and degree of cross-linking of fodrin on the cytoplasmic surface of the plasma membrane (see also reference 58). Thus, extensive cell–cell contact between MDCK cells may play a role in modulating the physiochemical properties, stability, and distribution of the fodrin-based membrane skeleton, which in turn may cause the lateral mobility of membrane proteins attached to the membrane skeleton to be more restricted and hence result in the maintenance of membrane domains in these regions of the cell. Since the degree of cell–cell contact and the distribution of integral and peripheral membrane proteins can be modulated experimentally in cultures of MDCK cells, it will be possible to test different aspects of this hypothesis in detail.

We are grateful to Ms. Sally Shepardson and Dr. Manfred Bayer (this institute) for the preparation and analysis of cells for electron microscopy; to Drs. Stephen Warren, Manijeh Pasdar, and Henry Parker for discussions during the course of this work and comments on the manuscript; and to Donna Buckley, Jan Krusen, and Denise Riley for typing the manuscript.

This work was supported by grants from the National Institutes of Health to Dr. Nelson (GM 35527) and the Institute for Cancer Research (CA-06927, RR-05539), and by an appropriation from the Commonwealth of Pennsylvania.

Received for publication 16 April 1986, and in revised form 23 June 1986.

Note Added in Proof: Immunofluorescence of sections of MDCK cells in continuous monolayers cut perpendicular to the substratum reveals α-fodrin staining predominantly at the basolateral domain of the plasma membrane and little or no staining of the apical domain.

References

1. Anderson, R. A., and R. E. Lourien. 1984. Glycophorin is linked by band 4.1 protein to the human erythrocyte membrane skeleton. *Nature (Lond.).* 307:655–658.
2. Anderson, R. A., and V. T. Marchesi. 1985. Regulation of the association of membrane skeletal protein 4.1 with glycophorin by a polyphosphoinositide. *Nature (Lond.).* 318:295–298.
3. Baines, A. J., and V. Bennett. 1985. Synapsin I is a spectrin-binding protein immunologically related to erythrocyte protein 4.1. *Nature (Lond.).* 315: 410–413.
4. Balcarova-Ständes, J., S. E. Pfeiffer, S. D. Fuller, and K. Simons. 1984. Development of cell surface polarity in the epithelial Madin-Darby Canine Kidney (MDCK) cell line. *EMBO (Eur. Mol. Biol. Organ.) J.* 3:2687–2694.
5. Bennett, V. 1985. The membrane skeleton of human erythrocytes and its implications for more complex cells. *Annu. Rev. Biochem.* 54:273–304.
6. Bennett, V., J. Davis, and W. A. Fowler. 1982. Brain spectrin, a membrane-associated protein related in structure and function to erythrocyte spectrin. *Nature (Lond.).* 299:126–131.
7. Bennett, V., and P. J. Stenbuck. 1979. Identification and partial purification of ankyrin, the high affinity membrane attachment site for human erythrocyte spectrin. *J. Biol. Chem.* 254:2533–2541.
8. Bennett, V., and P. J. Stenbuck. 1979. The membrane attachment protein for spectrin is associated with band 3 in human erythrocyte membranes. *Nature (Lond.).* 280:468–473.
9. Bennett, V., and P. J. Stenbuck. 1980. Association between ankyrin and the cytoplasmic domain of band 3 isolated from the human erythrocyte membrane. *J. Biol. Chem.* 255:2540–2548.
10. Bennett, V., A. J. Baines, and J. Q. Davis. 1985. Ankyrin and synapsin: Spectrin-binding proteins associated with brain membranes. *J. Cell. Biochem.* 29:157–169.
11. Ben-Ze'ev, A. 1984. Differential control of cytokeratins and vimentin synthesis by cell–cell contact and cell spreading in cultured epithelial cells. *J. Cell Biol.* 99:1424–1433.
12. Bologna, M., R. Allen, and R. Dulbecco. 1986. Organization of cytokeratin bundles by desmosomes in rat mammary cells. *J. Cell Biol.* 102:560–567.
13. Bonner, W. M., and R. A. Laskey. 1974. A film detection method for tritium-labeled proteins and nucleic acids in polyacrylamide gels. *Eur. J. Biochem.* 46:83–88.
14. Bourguignon, L. Y. W., S. J. Suchard, M. L. Nagpal, and J. R. Glenney. 1985. A T-lymphoma transmembrane glycoprotein (GP180) is linked to the cytoskeletal protein, fodrin. *J. Cell Biol.* 101:477–487.
15. Branton, D., C. M. Cohen, and J. Tyler. 1981. Interaction of cytoskeletal proteins on the human erythrocyte membrane. *Cell.* 24:24–32.
16. Burridge, K., T. Kelley, and P. Maugeat. 1982. Nonerythrocyte spectrin: actin-membrane attachment proteins occurring in many cell types. *J. Cell Biol.* 95:478–486.
17. Cereijido, M., E. S. Robbins, W. J. Dolan, C. A. Rotonno, and D. D. Sabatini. 1978. Polarized monolayers formed by epithelial cells on a permeable and translucent support. *J. Cell Biol.* 77:853–880.
18. Cereijido, M., J. Ehrenfeld, I. Meza, and A. Martinez-Palomo. 1980. Structural and functional membrane polarity in cultured monolayers of MDCK cells. *J. Membr. Biol.* 52:147–159.
19. Cereijido, M., I. Meza, and A. Martinez-Palomo. 1981. Occluding junctions in cultured epithelial monolayers. *Am. J. Physiol.* 240:C96–C102.
20. Cohen, C. M. 1983. The molecular organization of the red cell membrane skeleton. *Semin. Hematol.* 20:141–158.
21. DeCamilli, P., R. Cameron, and P. Greengard. 1983. Synapsin I (Protein I), a nerve terminal-specific phosphoprotein. I. Its general distribution in synapses of the central and peripheral nervous system demonstrated by immunofluorescence in frozen and plastic sections. *J. Cell Biol.* 96:1337–1354.
22. Drenckhahn, D., K. S. Schlülrt, D. P. Allen, and V. Bennett. 1985. Colocalization of Band 3 with ankyrin and spectrin at the basal membrane of intercalated cells in the rat kidney. *Science (Wash. DC).* 230:1287–1289.
23. Elgasaeter, A., D. M. Shotton, and D. Branton. 1976. Intramembrane particle aggregation in erythrocyte ghosts. II. The influence of spectrin aggregation. *Biochem. Biophys. Acta.* 426:101–122.
24. Feramisco, J. R., and K. Burridge. 1980. A rapid purification of α-actinin, filamin, and a 130,000-dalton protein from smooth muscle. *J. Biol. Chem.* 255:1194–1199.
25. Galli, P., A. Brenna, P. DeCamilli, and J. Meldolesi. 1976. Extracellular calcium and the organization of tight junctions in pancreatic animal cells. *Exp. Cell Res.* 99:178–183.
26. Geiger, B. 1985. Microfilament-membrane interaction. *Trends Biochem. Sci.* 10:456–461.
27. Glynn, I. M., and S. J. D. Karlish. 1975. The sodium pump. *Annu. Rev. Physiol.* 37:13–85.
28. Golan, D. E., and W. Veatch. 1980. Lateral mobility of band 3 in the human erythrocyte membrane studied by fluorescence photobleaching recovery: evidence for control by cytoskeletal interactions. *Proc. Natl. Acad. Sci. USA.* 77:2537–2541.
29. Glenney, J. R., and P. Glenney. 1983. Fodrin is the general spectrin-like protein found in most cells whereas spectrin and the TW protein have a restricted distribution. *Cell.* 34:503–512.
30. Glenney, J. R., and P. Glenney. 1984. Comparison of spectrin isolated from erythroid and non-erythroid sources. *Eur. J. Biochem.* 144:529–539.
31. Gonalez-Mariscal, L., B. Chávez de Ramírez, and M. Cereijido. 1985. Tight junction formation in cultured epithelial cells (MDCK). *J. Membr. Biol.* 86:113–125.
32. Griepp, E. B., W. J. Dolan, E. S. Robbins, and D. D. Sabatini. 1983. Participation of plasma membrane proteins in the formation of tight junctions by cultured epithelial cells. *J. Cell Biol.* 96:693–702.
33. Hertzlinger, D. A., and G. K. Ojakian. 1984. Studies on the development and maintenance of epithelial cell surface polarity with monoclonal antibodies. *J. Cell Biol.* 98:1777–1787.
34. Hoi-Sang, V., M. M. Saier, and M. M. Ellisman. 1979. Tight junction formation is closely linked to the polar redistribution of intramembranous particles in aggregating MDCK epithelia. *Exp. Cell Res.* 122:384–392.
35. Jones, J. C. R., and R. D. Goldman. 1985. Intermediate filaments and initiation of desmosome assembly. *J. Cell Biol.* 101:506–517.
36. Jørgensen, P. L. 1974. Purification and characterization of $(Na^+ + K^+)$-ATPase. III. Purification from the outer medulla of mammalian kidney after selective removal of membrane components by sodium dodecylsulfate. *Biochem. Biophys. Acta.* 356:36–52.
37. Jørgensen, P. L. 1982. Mechanisms of the Na^+, K^+ pump. Protein structure and conformation of the pure $(Na^+ + K^+)$-ATPase. *Biochim. Biophys. Acta.* 694:27–68.
38. Juliano, R. L., and A. Rothstein. 1971. Properties of an erythrocyte membrane lipoprotein fraction. *Biochim. Biophys. Acta.* 249:227–235.
39. Kellie, S., T. C. Holme, and M. J. Bissell. 1985. Interaction of tumor promoters with epithelial cells in culture: an immunofluorescence study. *Exp. Cell Res.* 160:259–274.
40. Kyte, J. 1976. Immunoferritin determination of the distribution of (Na^+, K^+)-ATPase over the plasma membranes or renal convoluted tubules. I. Distal segment. *J. Cell Biol.* 68:287–303.
41. Kyte, J. 1976. Immunoferritin determination of the distribution of (Na^+, K^+)-ATPase over the plasma membranes of renal convoluted tubules. II. Proximal segment. *J. Cell Biol.* 68:304–318.
42. Labarca, C., and K. Paigen. 1980. A simple, rapid, and sensitive DNA assay procedure. *Anal. Biochem.* 102:344–352.
43. Laemlli, U. K. 1970. Cleavage of structural proteins during the assembly of the head of bacteriophage T4. *Nature (Lond.).* 227:680–685.
44. Lamb, J. F., P. Ogden, and N. J. Simmons. 1981. Autoradiographic localization of [^{3}H]ouabain bound to cultured epithelial cell monolayers of MDCK cells. *Biochim. Biophys. Acta.* 644:333–340.
45. Laskey, R. A., and A. D. Mills. 1975. Quantitative detection of ^{3}H and ^{14}C in polyacrylamide gels by fluorography. *Eur. J. Biochem.* 56:335–341.
46. Lazarides, E., and W. J. Nelson. 1983. Expression of the erythrocyte form of spectrin in the cerebellum: existence of distinct membrane–cytoskeleton domains in neurons. *Science (Wash. DC).* 220:1295–1296.
47. Lazarides, E., W. J. Nelson, and T. Kasamatsu. 1984. Segregation of two spectrin forms in the chicken optic system: a mechanism for establishing restricted membrane-cytoskeletal domains in neurons. *Cell.* 36:269–278.
48. Lazarides, E., and W. J. Nelson. 1985. Expression and assembly of the erythroid membrane-skeletal proteins ankyrin (goblin) and spectrin in the morphogenesis of chicken neurons. *J. Cell. Biochem.* 27:423–441.
49. Lehto, V.-P., and I. Virtanen. 1983. Immunolocalization of a novel cytoskeleton-associated polypeptide of M_r 230,000 (p230). *J. Cell Biol.* 96:703–716.
50. Levine, J., and M. Willard. 1981. Fodrin: axonally transported polypeptides associated with the internal periphery of many cells. *J. Cell Biol.* 90:631–643.
51. Levine, J., and M. Willard. 1983. Redistribution of fodrin (a component of the cortical cytoplasm) accompanying capping of cell surface molecules. *Proc. Natl. Acad. Sci. (USA).* 80:191–195.
52. Louvard, D. 1980. Apical membrane aminopeptidase appears at the site of cell–cell contact in cultured kidney epithelial cells. *Proc. Natl. Acad. Sci. USA.* 77:4132–4136.
53. Lux, S. E., K. M. John, and M. J. Karnovsky. 1976. Irreversible deformation of the spectrin-actin lattice in irreversibly sickled cells. *J. Clin. Invest.* 58:955–963.
54. Marchesi, V. T., and E. Steers. 1968. Selective solubilization of a protein component of the red cell membrane. *Science (Wash. DC).* 159:203–204.
55. Madin, S. J., and N. B. Darby. 1979. American Type Culture Collection Catalogue of Strains II. p. 30.
56. Matlin, K. S., and K. Simons. 1984. Sorting of an apical plasma membrane glycoprotein occurs before it reaches the cell surface in cultured epithelial cells. *J. Cell Biol.* 99:2131–2139.
57. Matsuura, S., H. Nakada, T. Sawamura, and Y. Tashiro. 1982. Redistribution of an asialoglycoprotein receptor on rat hepatocyte cell surface. *J. Cell Biol.* 95:864–875.
58. McCloskey, M., and M-m. Poo. 1984. Protein diffusion in cell membranes: some biological implications. *Int. Rev. Cytol.* 87:19–80.

59. Meza, I., G. Ibarra, M. Sabamero, A. Martinez-Paloma, and M. Cereijido. 1980. Occluding junctions and cytoskeletal components in a cultured transporting epithelium. *J. Cell Biol.* 87:746–754.

60. Misek, D. E., E. Bard, and E. Rodriguez-Boulan. 1984. Biogenesis of epithelial cell polarity: intracellular sorting and vectorial exocytosis of an apical plasma membrane glycoprotein. *Cell.* 59:537–546.

61. Misfeldt, D. S., S. T. Hammanmoka, and D. R. Pitelka. 1976. Transepithelial transport in cell culture. *Proc. Natl. Acad. Sci. USA.* 73:1212–1215.

62. Mueller, H., and W. W. Franke. 1983. Biochemical and immunological characterization of desmoplakins I and II, the major polypeptides of the desmosomal plaque. *J. Mol. Biol.* 163:647–671.

63. Nelson, W. J., C. E. Vorgias, and P. Traub. 1982. A rapid method for the large-scale purification of the intermediate filament protein vimentin by single-stranded DNA–cellulose affinity chromatography. *Biochem. Biophys. Res. Commun.* 106:1141–1147.

64. Nelson, W. J., and E. Lazarides. 1983. Switching of the subunit composition of muscle spectrin during myogenesis *in vitro. Nature (Lond.).* 304:364–368.

65. Nelson, W. J., and E. Lazarides. 1983. Expression of β-spectrin in nonerythroid cells. *Proc. Natl. Acad. Sci. USA.* 80:363–367.

66. Nelson, W. J., B. L. Granger, and E. Lazarides. 1983. Avian lens spectrin: subunit composition compared with erythrocyte and brain spectrins. *J. Cell Biol.* 97:1271–1276.

67. Nelson, W. J., and E. Lazarides. 1984. The pattern of expression of two goblin (ankyrin) isoforms in chicken nervons reveals distinct steps in the assembly of the membrane-skeleton in neuronal morphogenesis. *Cell.* 39:309–320.

68. Nelson, W. J., and E. Lazarides. 1984. Assembly and establishment of membrane-cytoskeleton domains during differentiation: spectrin as a model system. *In* Cell Membranes: Methods and Reviews. Vol. 2. E. Elson, W. Frazier, and L. Glaser, editors. 219–246.

69. Nelson, W. J., C. A. L. S. Colaco, and E. Lazarides. 1983. Involvement of spectrin in cell-surface receptor capping in lymphocytes. *Proc. Natl. Acad. Sci. USA.* 80:1626–1630.

70. Noda, H. 1960. Physico-chemical studies on the soluble collagen of rat-tail tendon. *Biochim. Biophys. Acta.* 17:92–98.

71. Overton, J., and R. DeSalle. 1980. Control of desmosome formation in aggregating embryonic chick cells. *Dev. Biol.* 75:168–176.

72. Parr, E. L., and W. N. Kirby. 1979. Immunoferritin labeling study of M-2-antigens on dissociated epithelial cells. *J. Histochem. Cytochem.* 27:1327–1336.

73. Perrin, D., and D. Auris. 1985. Reorganization of α-fodrin induced by stimulation in secretory cells. *Nature (Lond.).* 315:589–592.

74. Pesonen, M., and K. Simons. 1983. Transepithelial transport of a viral membrane glycoprotein implanted into the apical plasma membrane of Madin-Darby Canine Kidney cells. I. Morphological evidence. *J. Cell Biol.* 97:627–637.

75. Pfeiffer, S., S. D. Fuller, and K. Simons. 1985. Intracellular sorting and basolateral appearance of the G protein of vesicular stomatitis virus in Madin-Darby Canine Kidney cells. *J. Cell Biol.* 101:470–476.

76. Pisam, M., and P. Ripoche. 1976. Redistribution of surface macromolecules in dissociated epithelial cells. *J. Cell Biol.* 71:907–920.

77. Pratt, B. M., A. S. Harris, J. S. Morrow, and J. A. Madri. 1984. Mechanisms of cytoskeletal regulation, modulation of aortic endothelial cell spectrin by the extra cellular matrix. *Am. J. Pathol.* 117:349–354.

78. Repasky, E. A., B. L. Granger, and E. Lazarides. 1982. Widespread occurrence of avian spectrin in nonerythroid cells. *Cell.* 29:821–833.

79. Rindler, M. J., I. E. Ivanov, H. Plesken, and D. D. Sabatini. 1985. Polarized delivery of viral glycoproteins to the apical and basolateral plasma membranes of Madin-Darby Canine Kidney cells infected with temperature-sensitive viruses. *J. Cell Biol.* 100:136–151.

80. Rodriguez, J., and F. Deinhardt. 1960. Preparation of a semipermanent mounting medium for fluorescent antibody studies. *Virology.* 12:316–317.

81. Rodriguez-Boulan, E. 1983. Membrane biogenesis, enveloped RNA viruses, and epithelial polarity. *Mod. Cell Biol.* 1:119–170.

82. Rodriguez-Boulan, E., K. T. Paskiet, and D. D. Sabatini. 1983. Assembly of enveloped viruses in MDCK cells: polarized budding from single attached cells and from clusters of cells in suspension. *J. Cell Biol.* 96:866–874.

83. Saier, M. H. 1981. Growth and differentiation properties of a kidney epithelial cell line (MDCK). *Am. J. Physiol.* 240:C106–C109.

84. Sang, V. H., M. H. Saier, and M. H. Ellisman. 1979. Tight junction formation is closely linked to the polar redistribution of intramembranous particles in aggregating MDCK epithelia. *Exp. Cell Res.* 122:384–391.

85. Sheetz, M. P., P. Febbroriello, and D. E. Koppel. 1982. Triphosphinositide increases glycoprotein lateral mobility in erythrocyte membranes. *Nature (Lond.).* 296:91–93.

86. Simons, K., and S. D. Fuller. 1985. Cell surface polarity in epithelia. *Annu. Rev. Cell Biol.* 1:243–288.

87. Steck, T. L., and J. Yu. 1973. Selective solubilization of proteins from red blood cell membranes by protein perturbants. *J. Supramol. Struct.* 1:220–232.

88. Towbin, H., T. Staehelin, and J. Gordon. 1979. Electrophoretic transfer of proteins from polyacrylamide gels to nitrocellulose sheets: procedure and some applications. *Proc. Natl. Acad. Sci. USA.* 76:4350–4354.

89. Tyler, J., W. Hargreaves, and D. Branton. 1979. Purification of two spectrin binding proteins: biochemical and electron microscopic evidence for site-specific reassociation between bands 2.1 and 4.1 to spectrin. *J. Biol. Chem.* 255:7034–7039.

90. Valentich, J. D., R. Tchao, and J. Leighton. 1979. Hemicyst formation stimulated by cyclic AMP in dog kidney cell line (MDCK). *J. Cell Physiol.* 100:291–304.